Part III

Early stages in stellar evolution

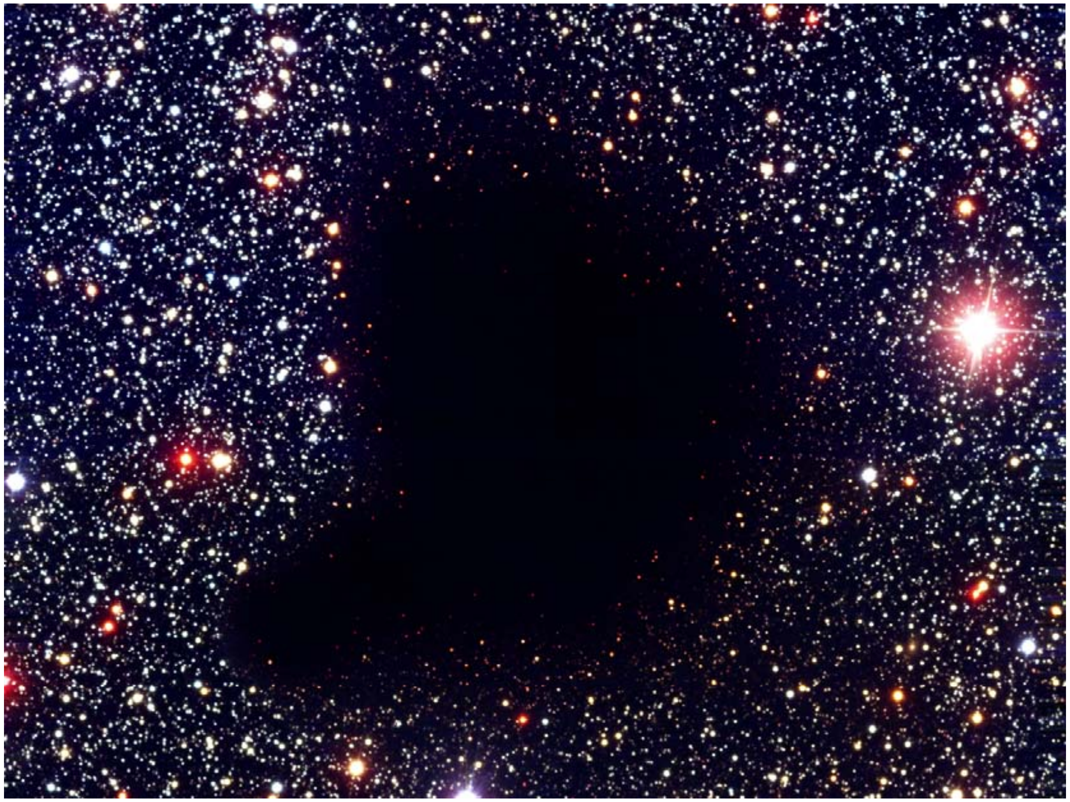

B68 with VLT/FORS1

PhD course originally developed by René Liseau
Updated to Master level course by Alexis Brandeker

Early stages in stellar evolution

- L15 – General Overview / Pre-collapse phase I
- L16 – Pre-collapse phase II
- L17 – Collapse phase I
- **L18 – Collapse phase II**
- L19 – Circumstellar disks I
- L20 – Pre-main-sequence evolution
- L21 – Circumstellar disks II – debris disks

Numerical model of collapse

- Simulation by Bate, Bonnell, & Bromm (2002)
- Newer 3D simulation (at the end) by Bate (2007)

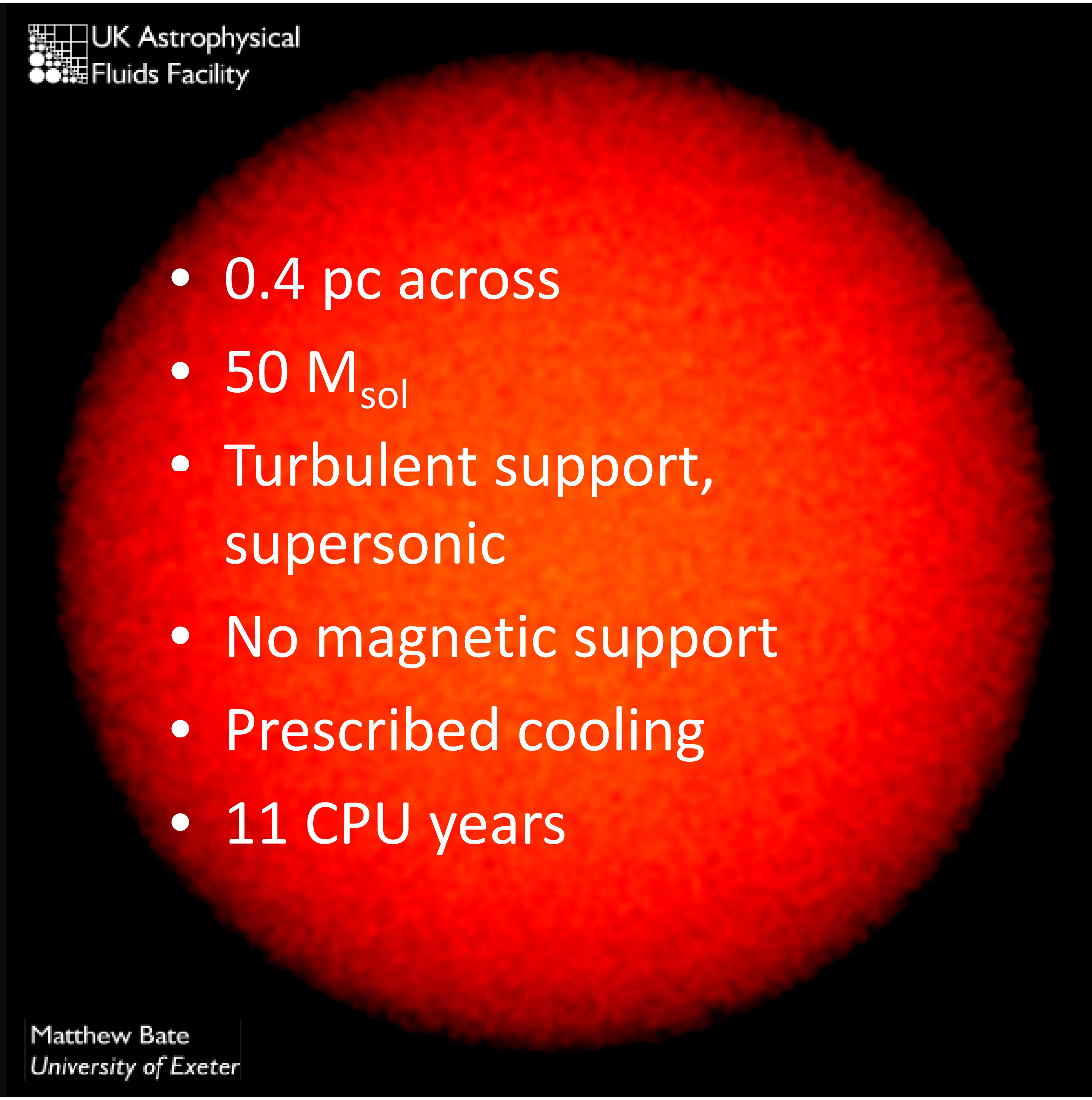

- 0.4 pc across
- 50 M_{sol}
- Turbulent support, supersonic
- No magnetic support
- Prescribed cooling
- 11 CPU years

- Shockwaves

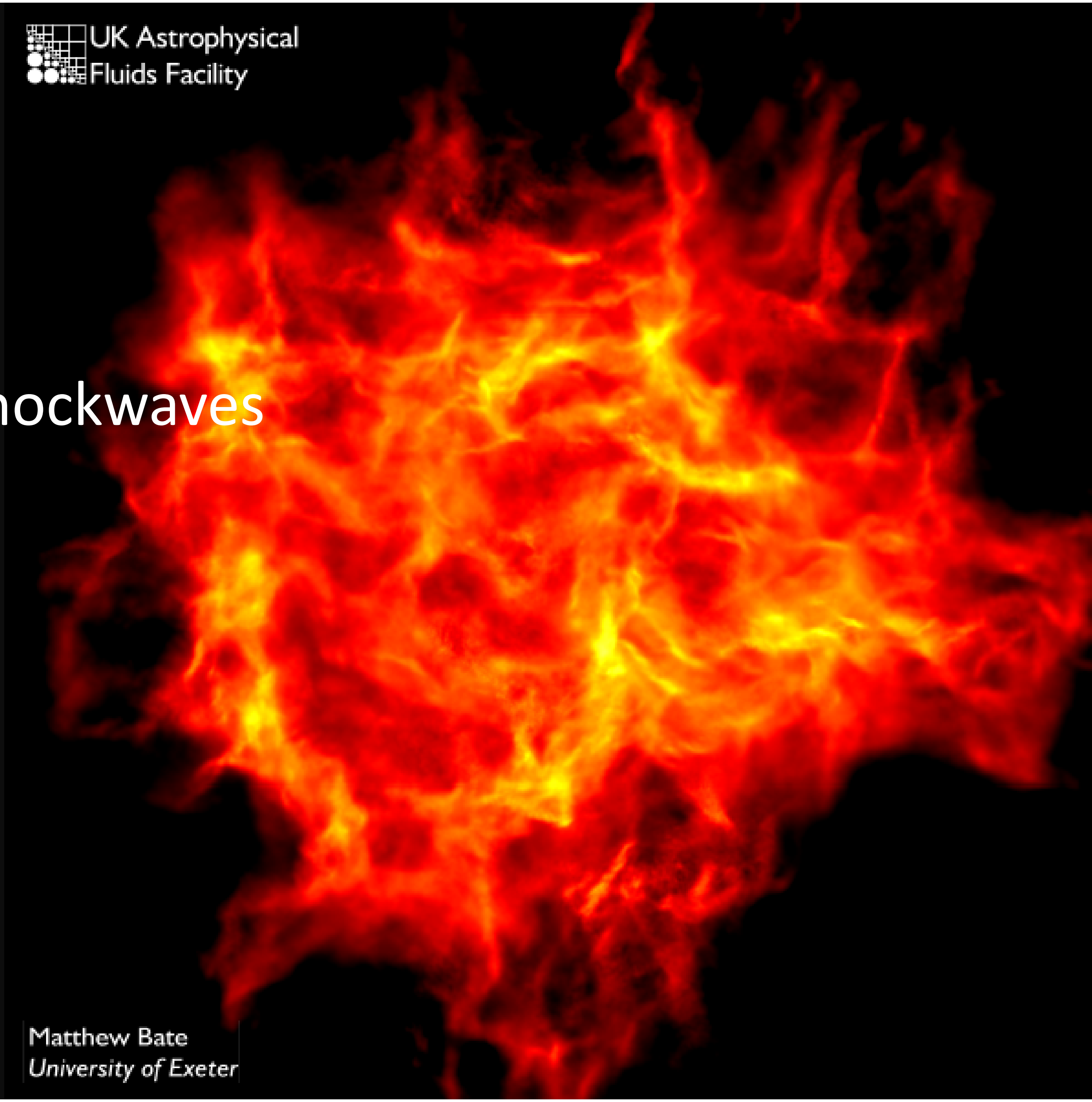
UK Astrophysical
Fluids Facility
Matthew Bate
University of Exeter

- Energy loss → gravity takes over

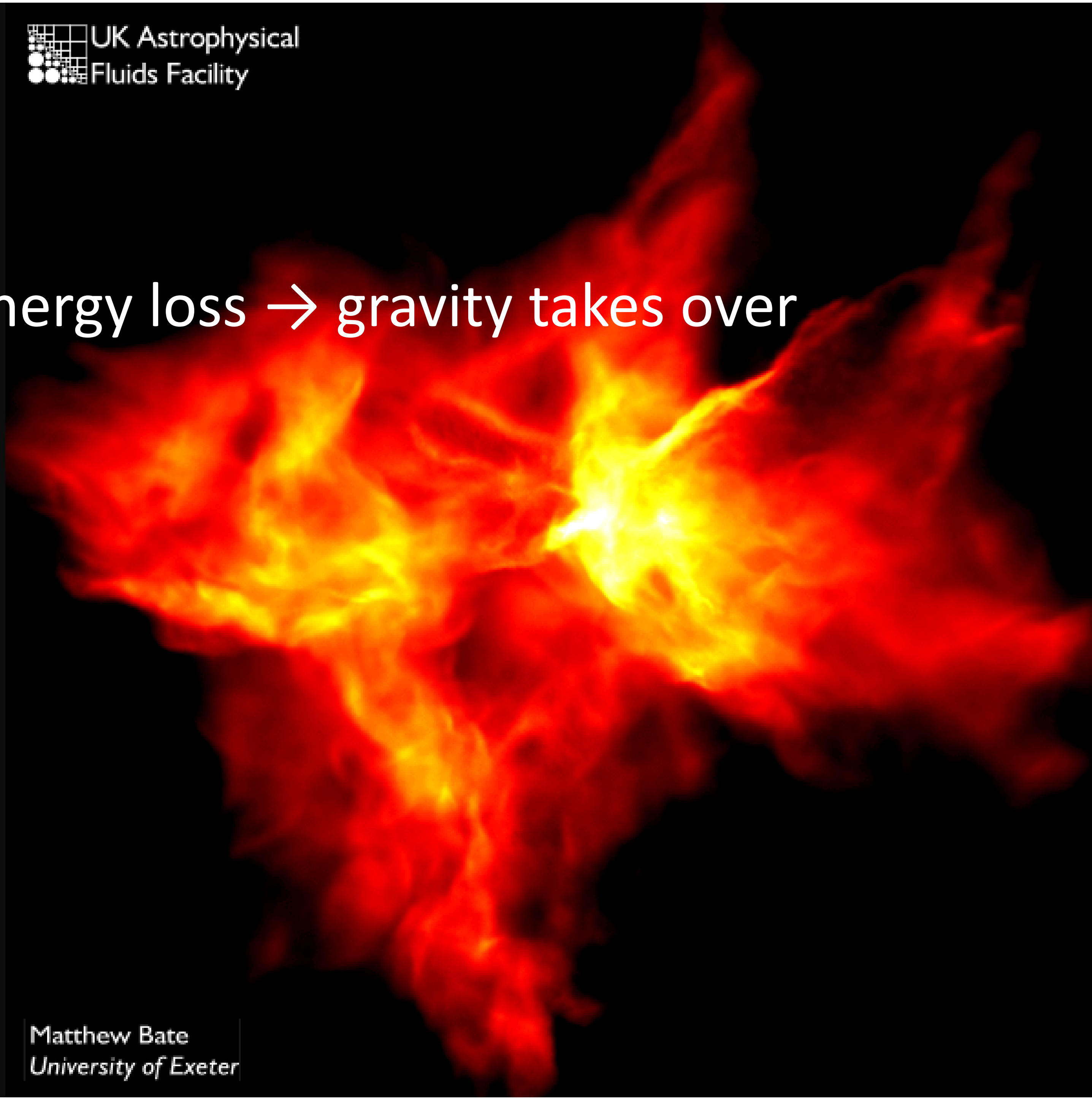

- Stars and brown dwarf form

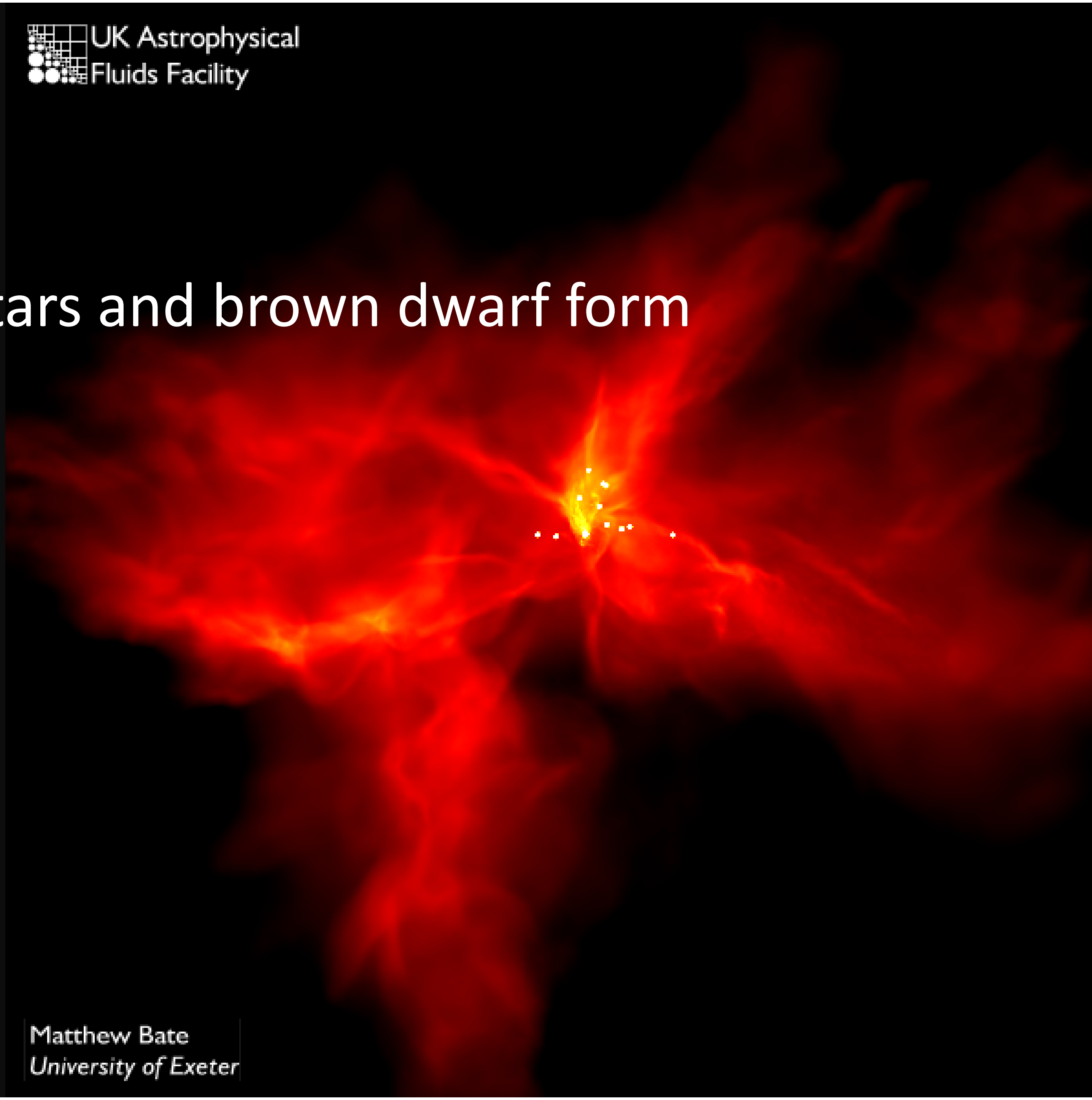

- Dynamical interactions → some ejections

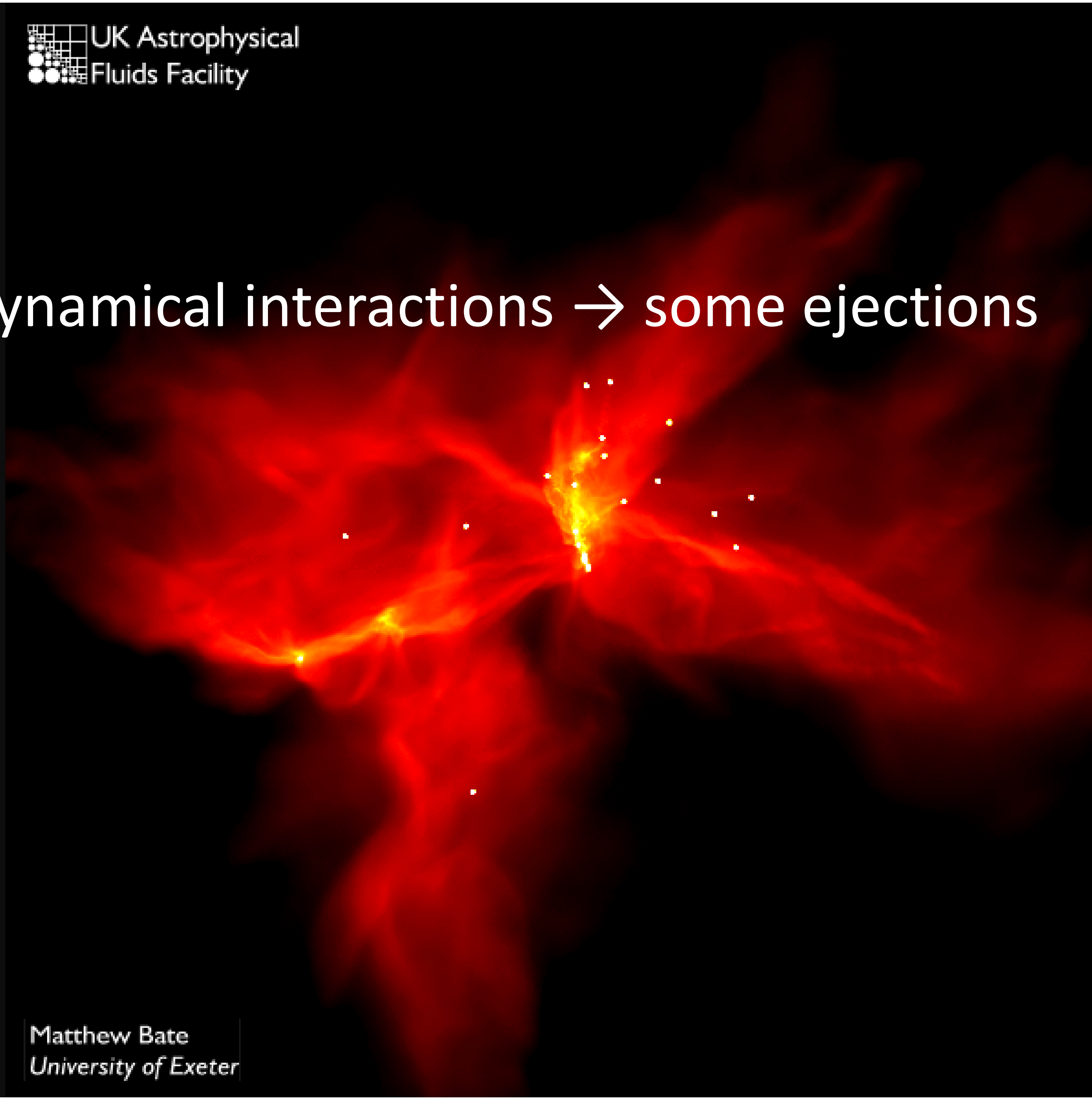

- End of simulation: some objects ejected from star forming region

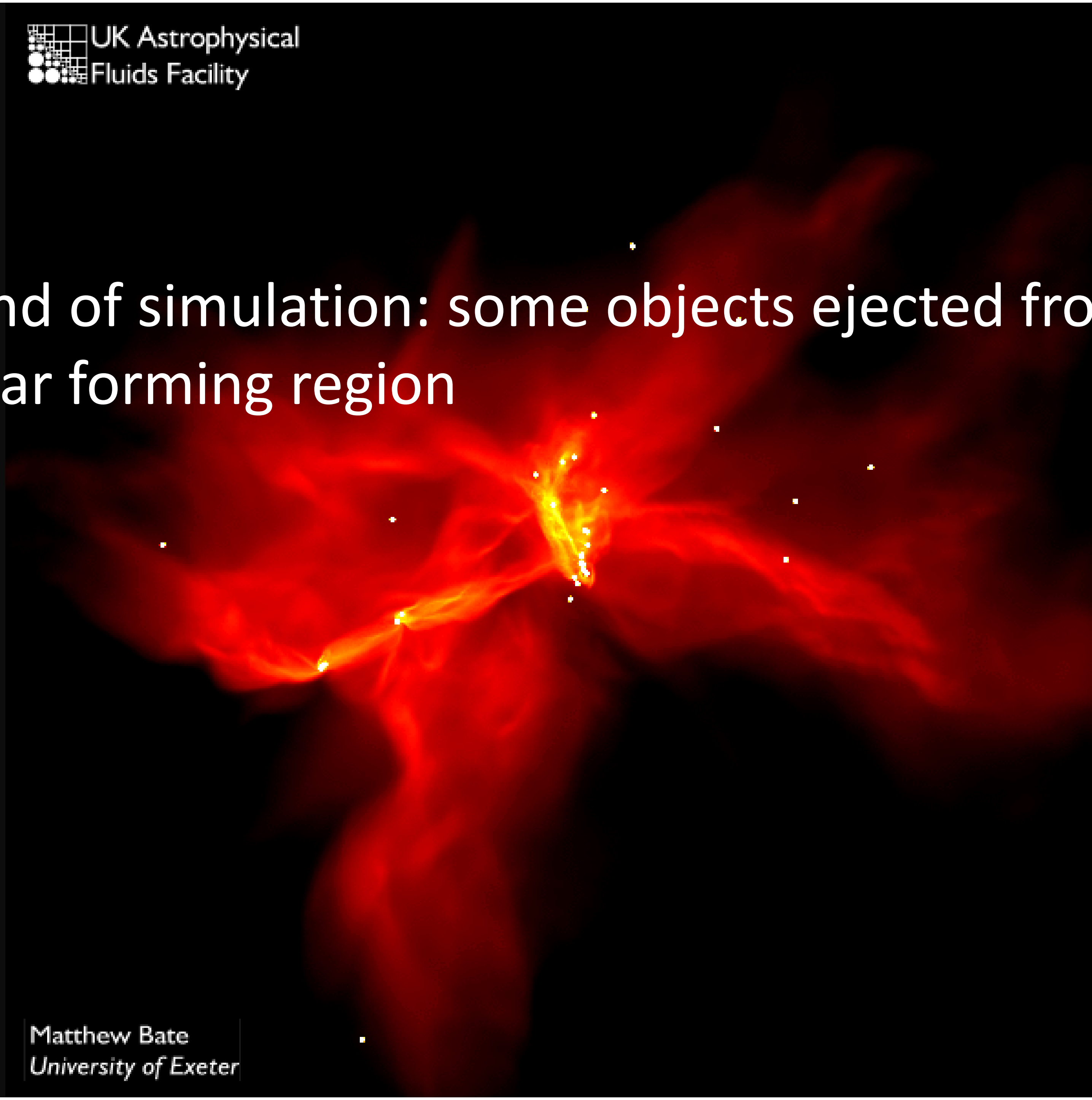

- Detail (5100 AU across): Formation of binary

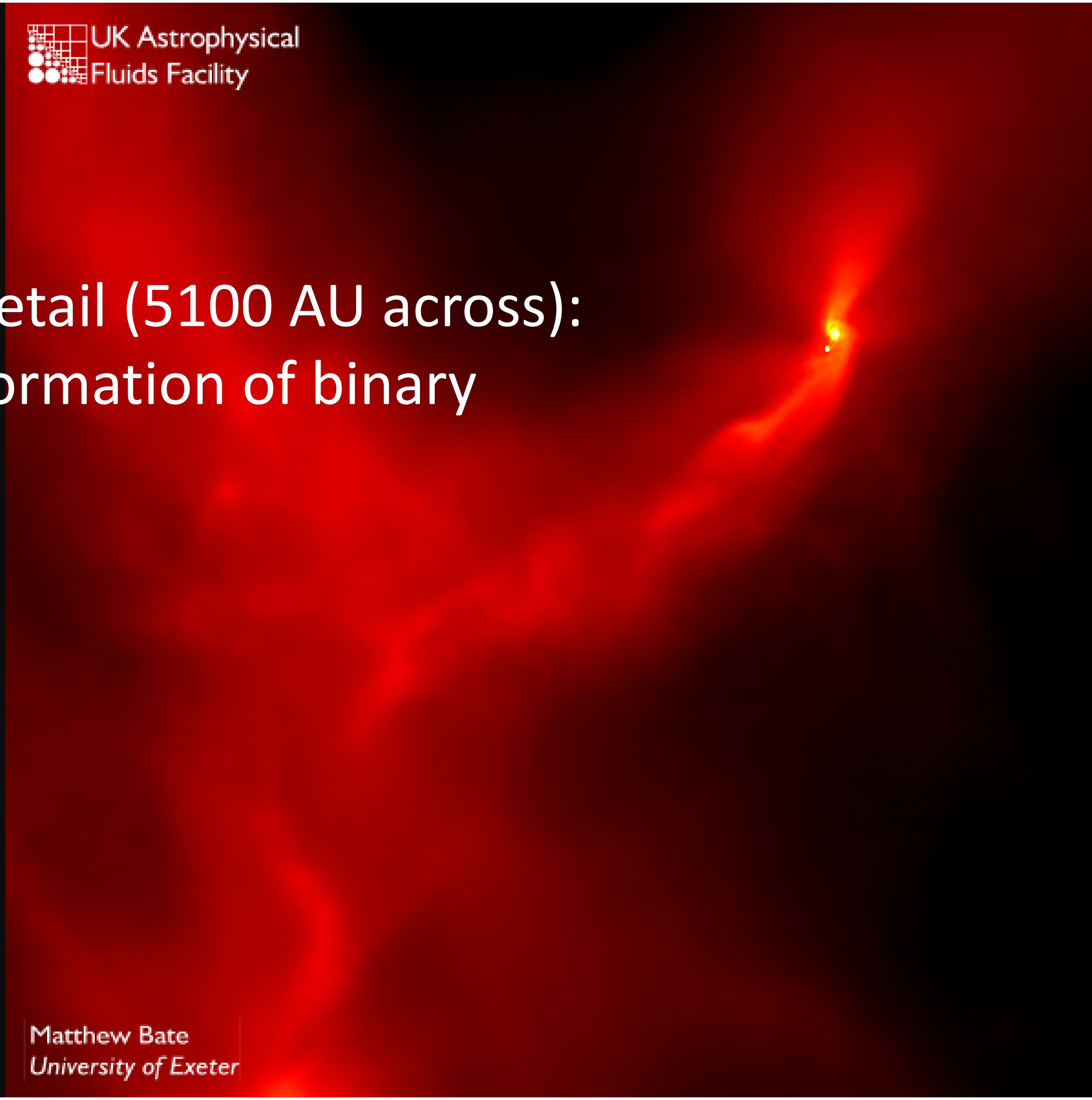

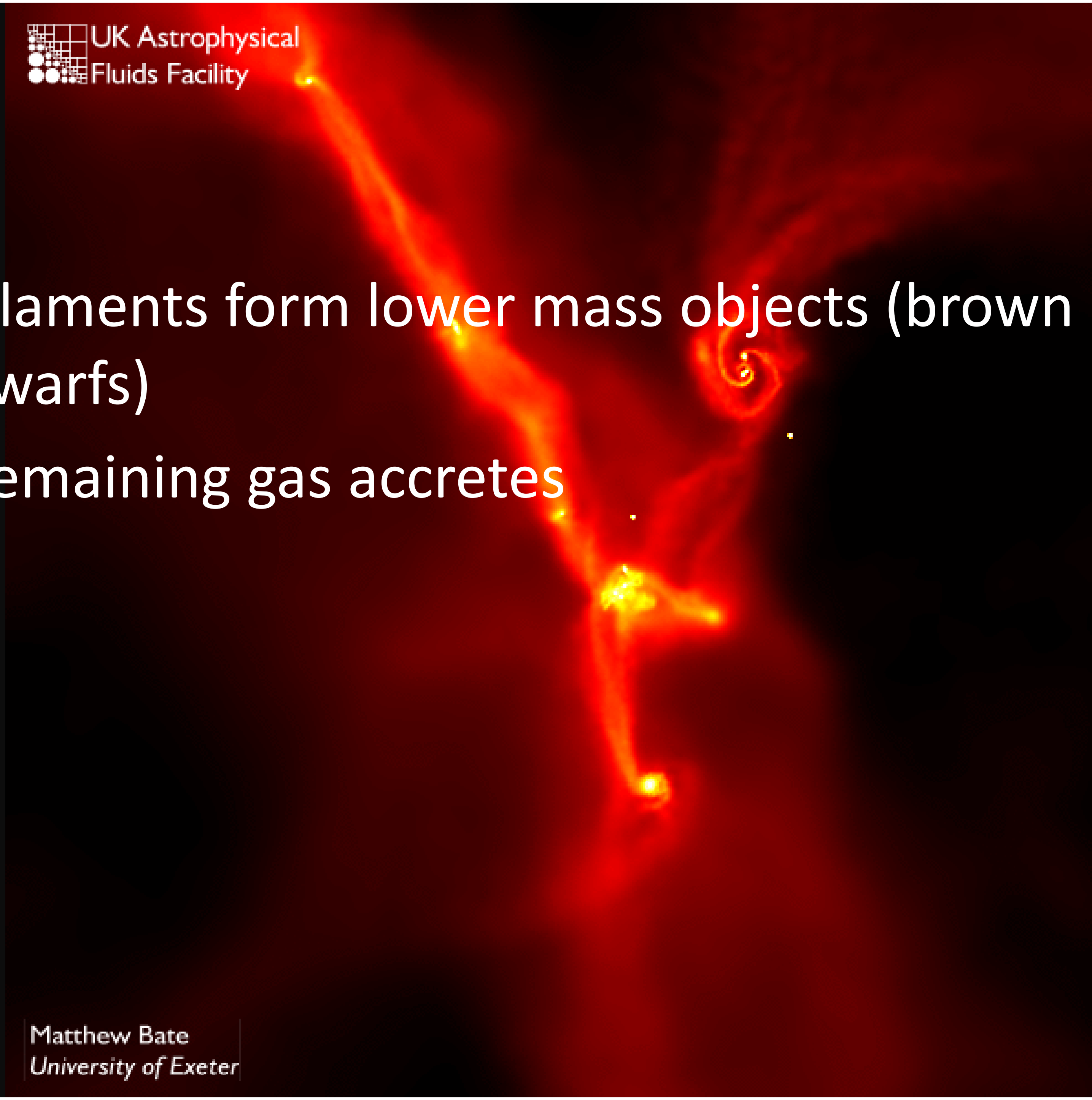

- Filaments form lower mass objects (brown dwarfs)
- Remaining gas accretes

- Objects dynamically interact
- Object with edge-on disk gets ejected

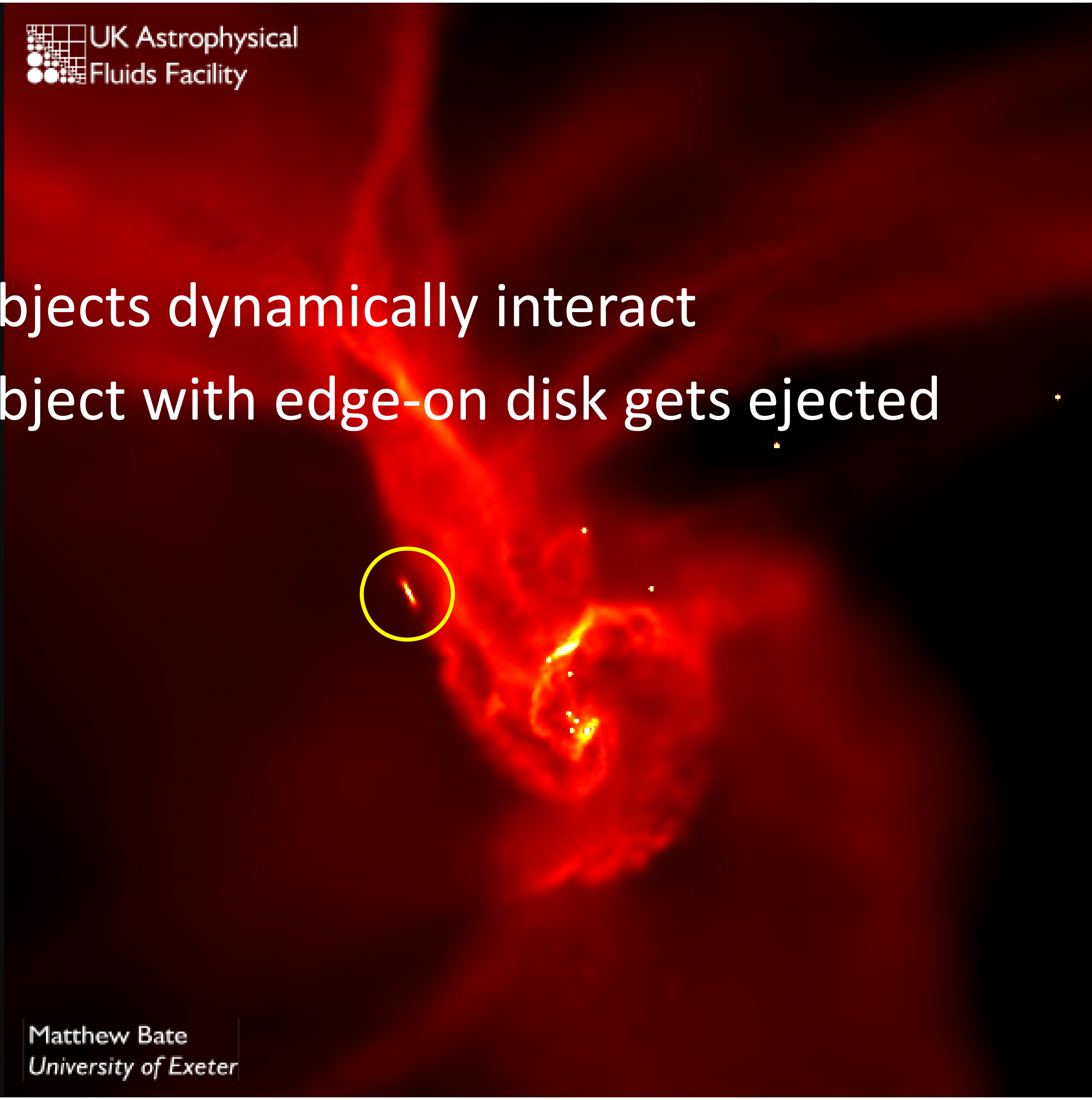

- Unstable quintuple system breaks apart and scatters

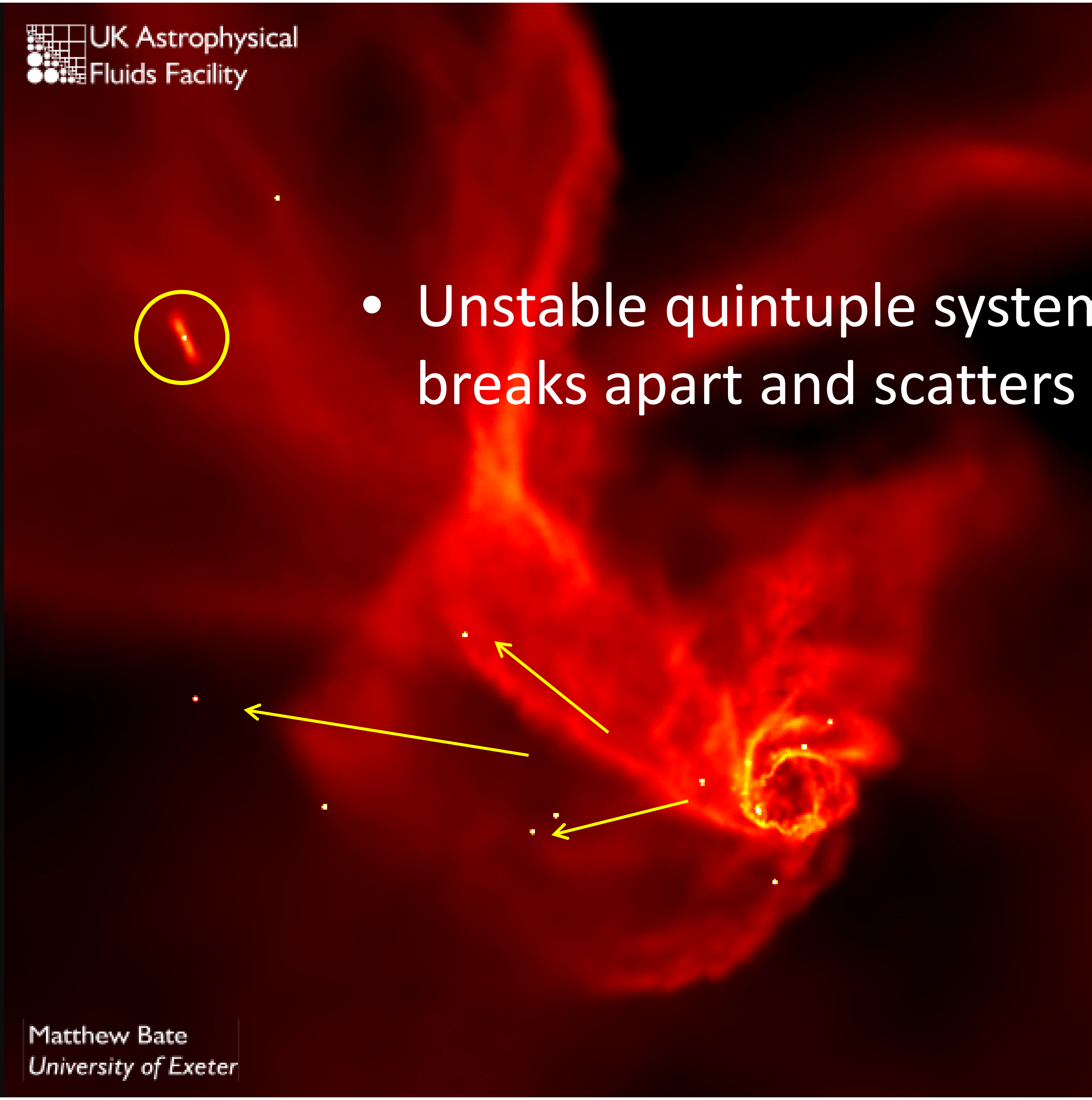

- Star formation proceeds in the accretion disk

- Objects formed in disks dynamically unstable, become ejected

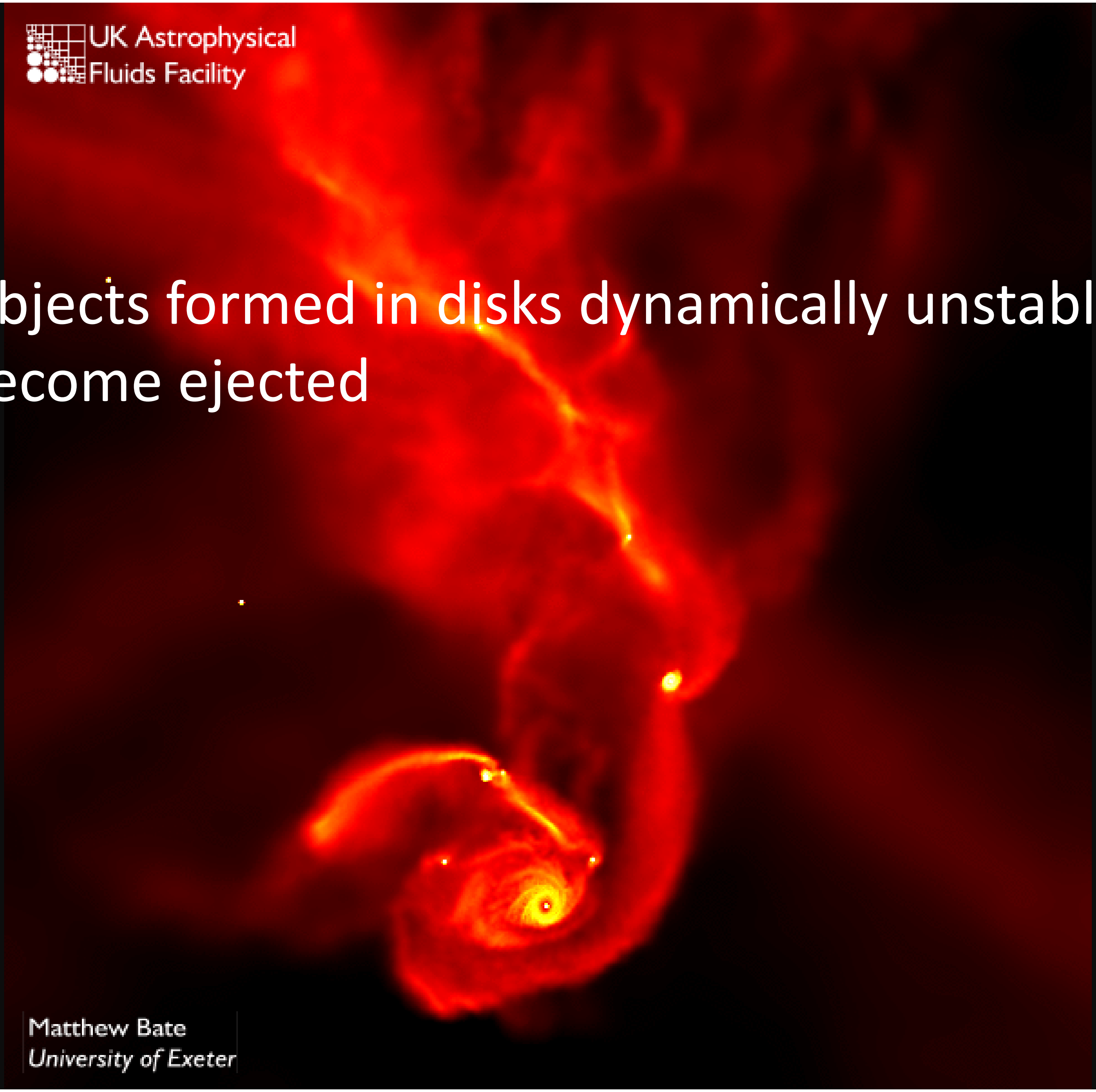

- Newly formed objects get their own accretion disks, truncated in encounters

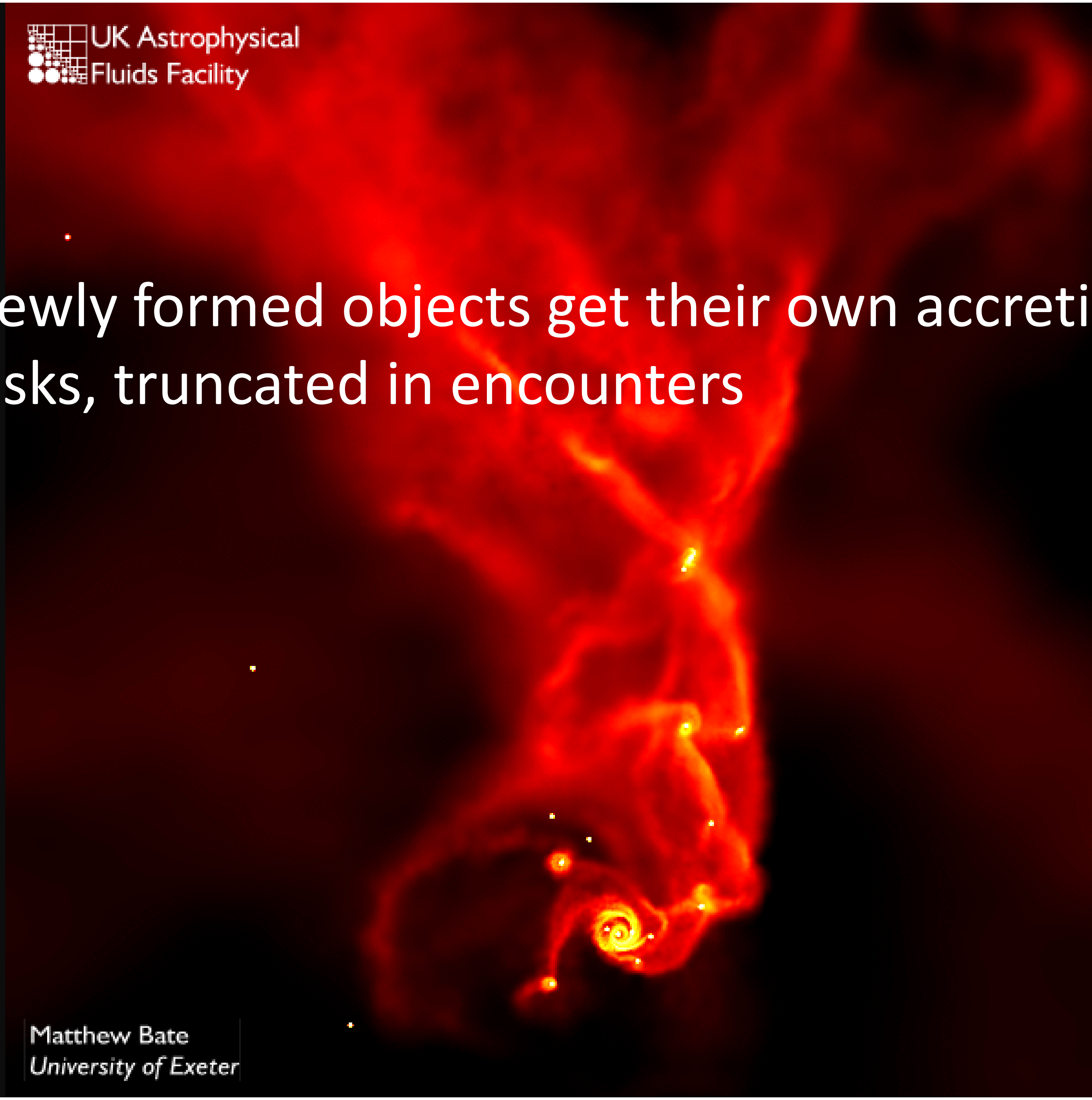

- Brown dwarf with disk gets ejected

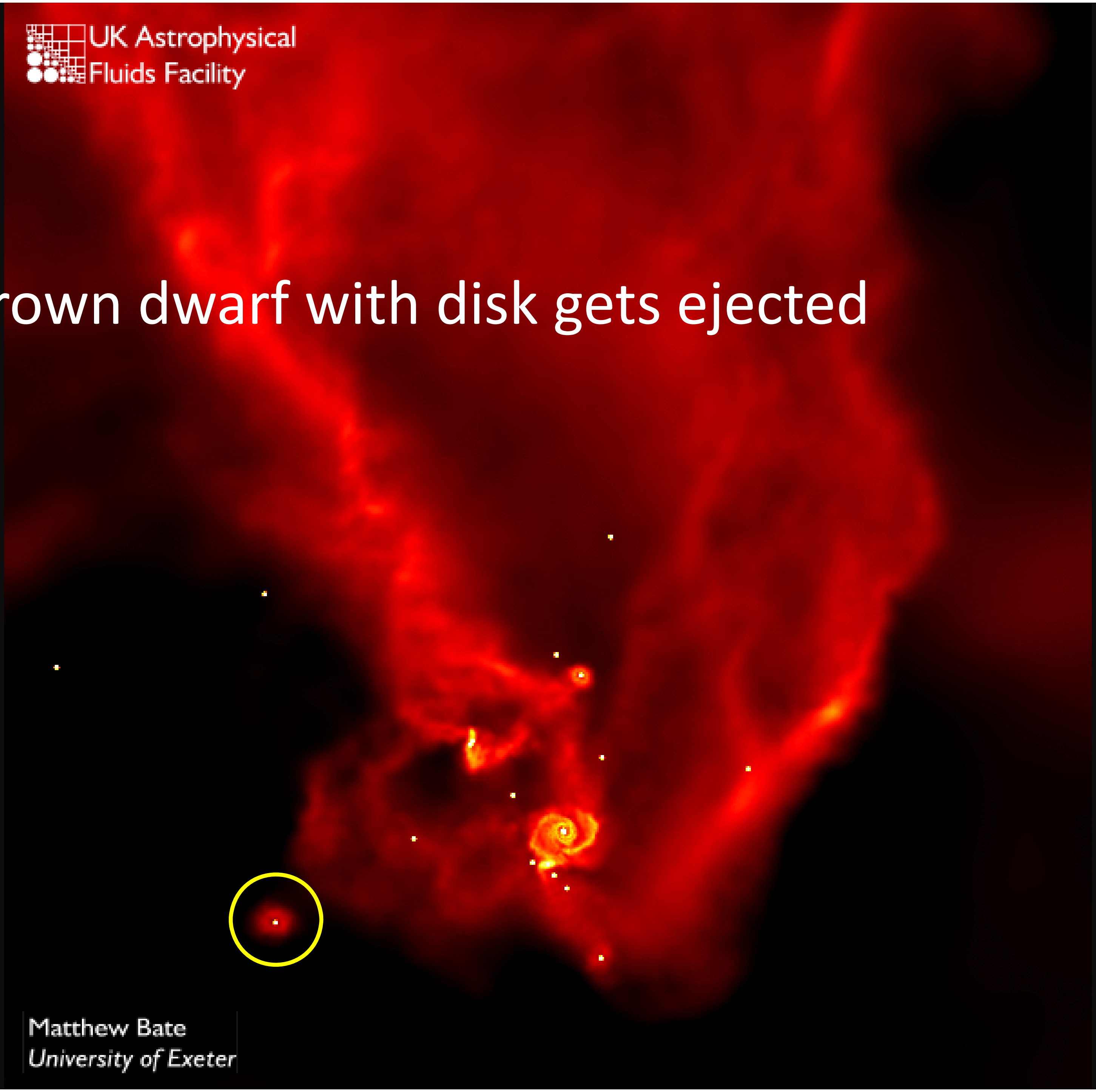

- Detail of main star-forming region at end of simulation

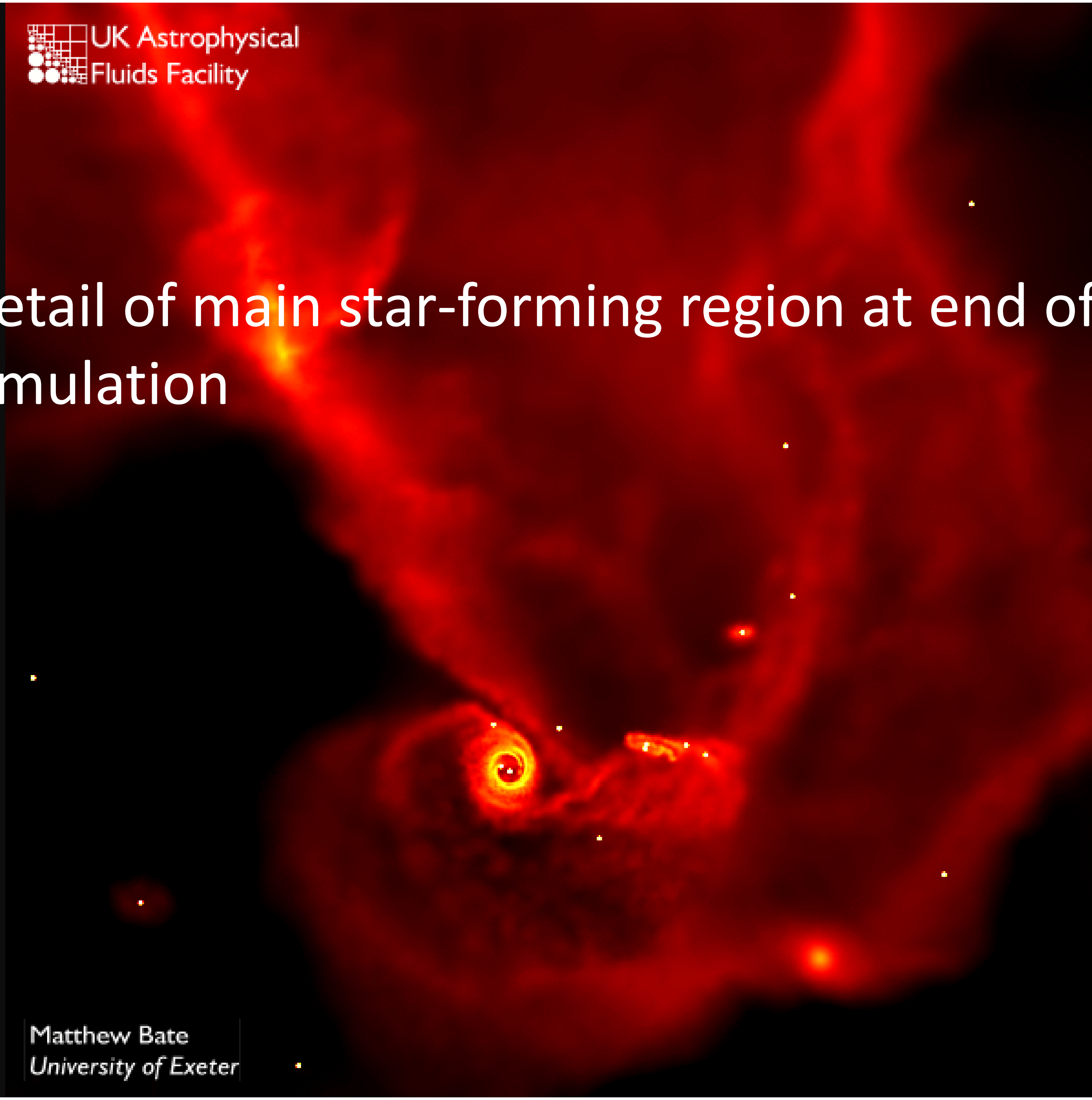

Detecting star formation

- Predictions from theory:

(a) mass $M > M_J \approx$ a few M_o

$$(\text{dense}: M_J \propto \rho^{-1/2}, \text{cold}: M_J \propto T^{3/2})$$

(b) length $R > \lambda_J \approx$ a fraction of a pc (for a few M_o)

(c) a velocity field $\quad v(r) \propto r^{-\alpha}$ [e.g., $\alpha = 0.5$]

(d) a density distribution $\quad \rho(r) \propto r^{-\beta}$ [e.g., $\beta = 1.5$ to 2]

Detecting star formation

(a) mass and (b) length $\Rightarrow$

[1] column density : $N(\mathrm{H}) = \int n(\mathrm{H})dl > 12\times10^{21}\,\mathrm{cm}^{-2}$ $[n(\mathrm{H}_2) = 10^4\,\mathrm{cm}^{-3}, L = 0.2\mathrm{pc}]$

of gas + dust $\Rightarrow A_\mathrm{V} \geq 12$ mag

extinction : $(I/I_0)_\mathrm{V} = e^{-\tau_\mathrm{V}} < 10^{-5}$

$\Rightarrow$ IR : $A_\lambda < 0.1A_\mathrm{V}$ for $\lambda > 2\mu\mathrm{m}$

[2] temperature : $T < 10^3\,\mathrm{K}$

$\Rightarrow$ IR : $\lambda > 3\mu\mathrm{m}$

$$\boxed{\begin{array}{l} N(\mathrm{H\,I} + 2\mathrm{H}_2) = 1.9\times10^{21}\,A_\mathrm{V}\,\mathrm{cm}^{-2} \\ A_\lambda = 1.086\,\tau_\lambda \approx \tau_\lambda \end{array}}$$

Radiation to look for

- Continuum radiation
  - From protostellar photospheres
  - Free-free gas emission
  - *Thermal radiation from radiatively heated dust grains*
- Line radiation
  - Cold gas → low-state molecular transitions

Continuum radiation

- Large optical depths & T < 1000 K
  → long wavelengths

- To infer total mass, one needs gas/dust relation. Generally assumed:

$$\boldsymbol{m_{gas}/m_{dust} = 100}$$

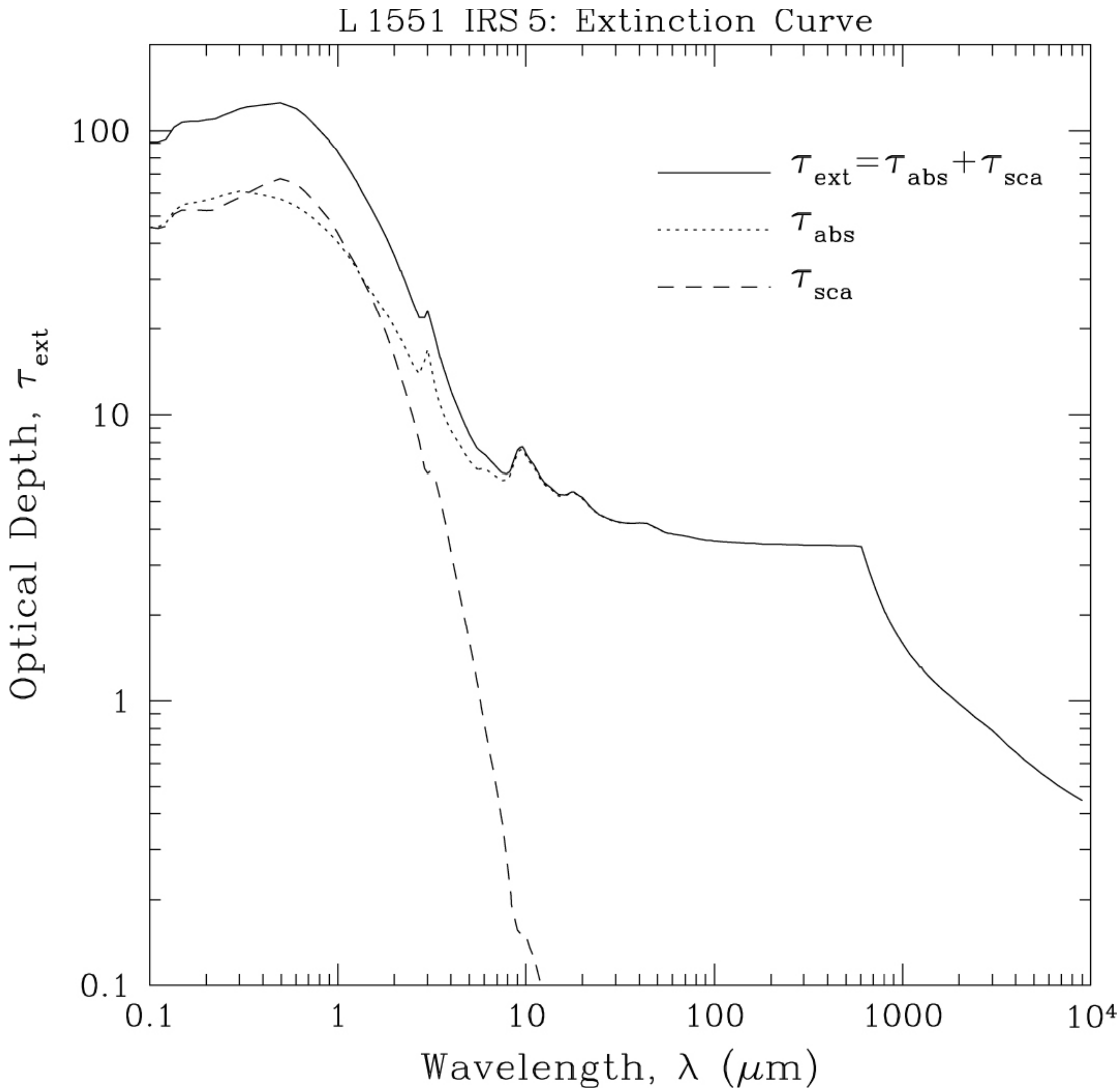

L 1551 IRS 5: Extinction Curve
$\tau_{ext} = \tau_{abs} + \tau_{sca}$
τ_{abs}
τ_{sca}
Optical Depth, τ_{ext}
100
10
1
0.1
0.1
1
10
100
1000
10^4
Wavelength, λ (μm)

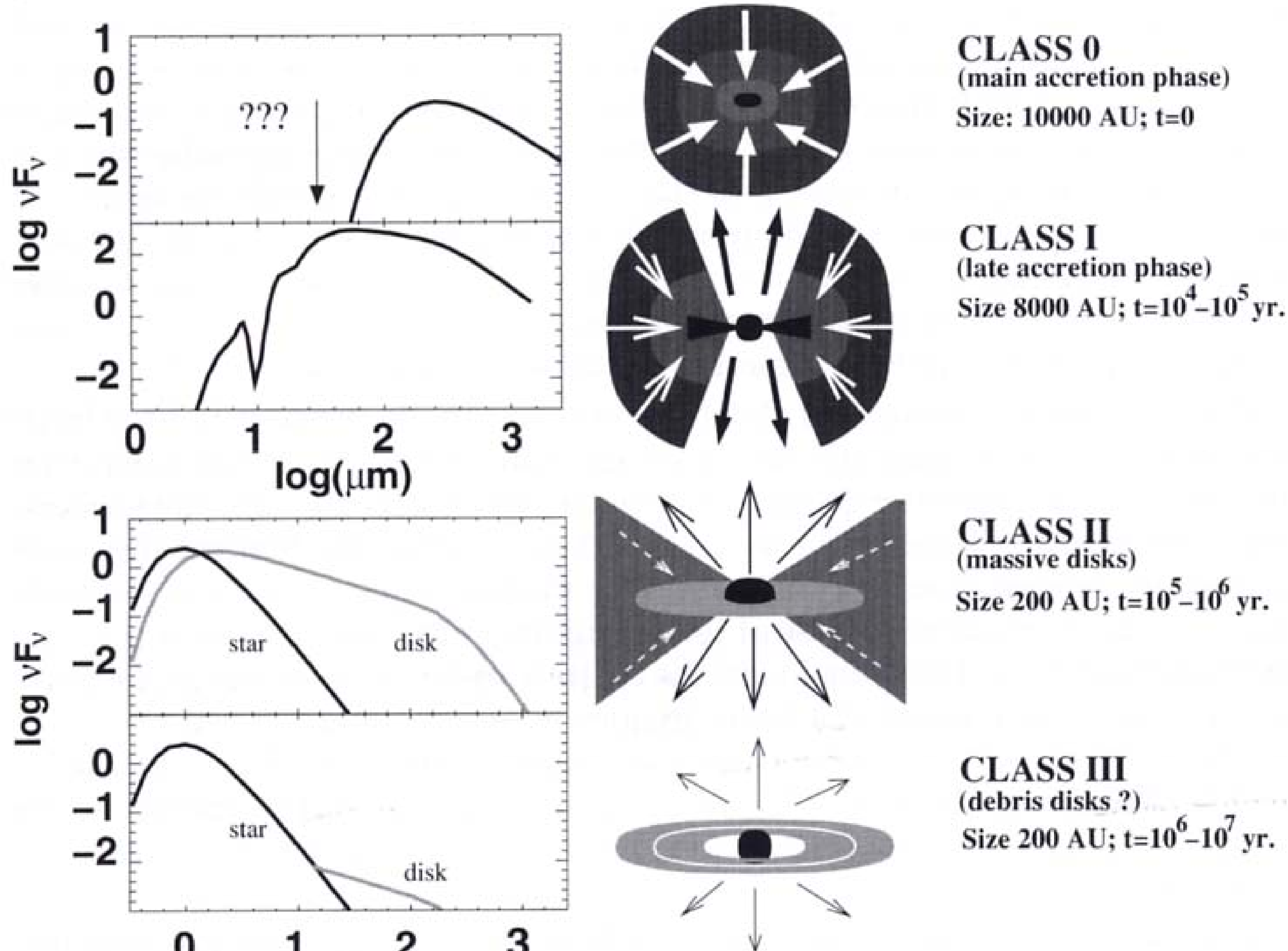

Adapted from van Zadelhoff 2002, PhD thesis

Spectral Energy Distributions (SEDs)

SED fitting

Observations

+

Theoretical models

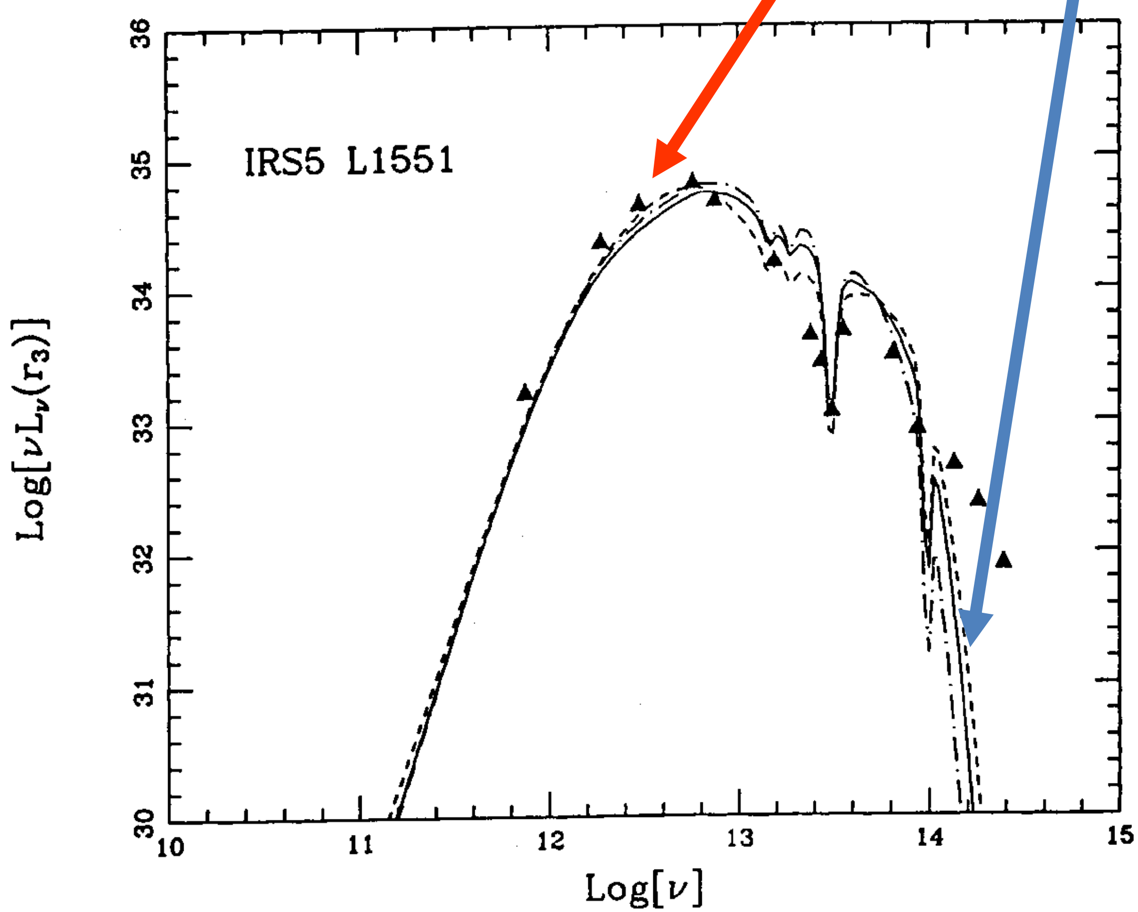

Adams, Lada & Shu 1987ApJ 312, 788

Spatial Profile fitting

Observations

Azimuthal Intensity Distribution

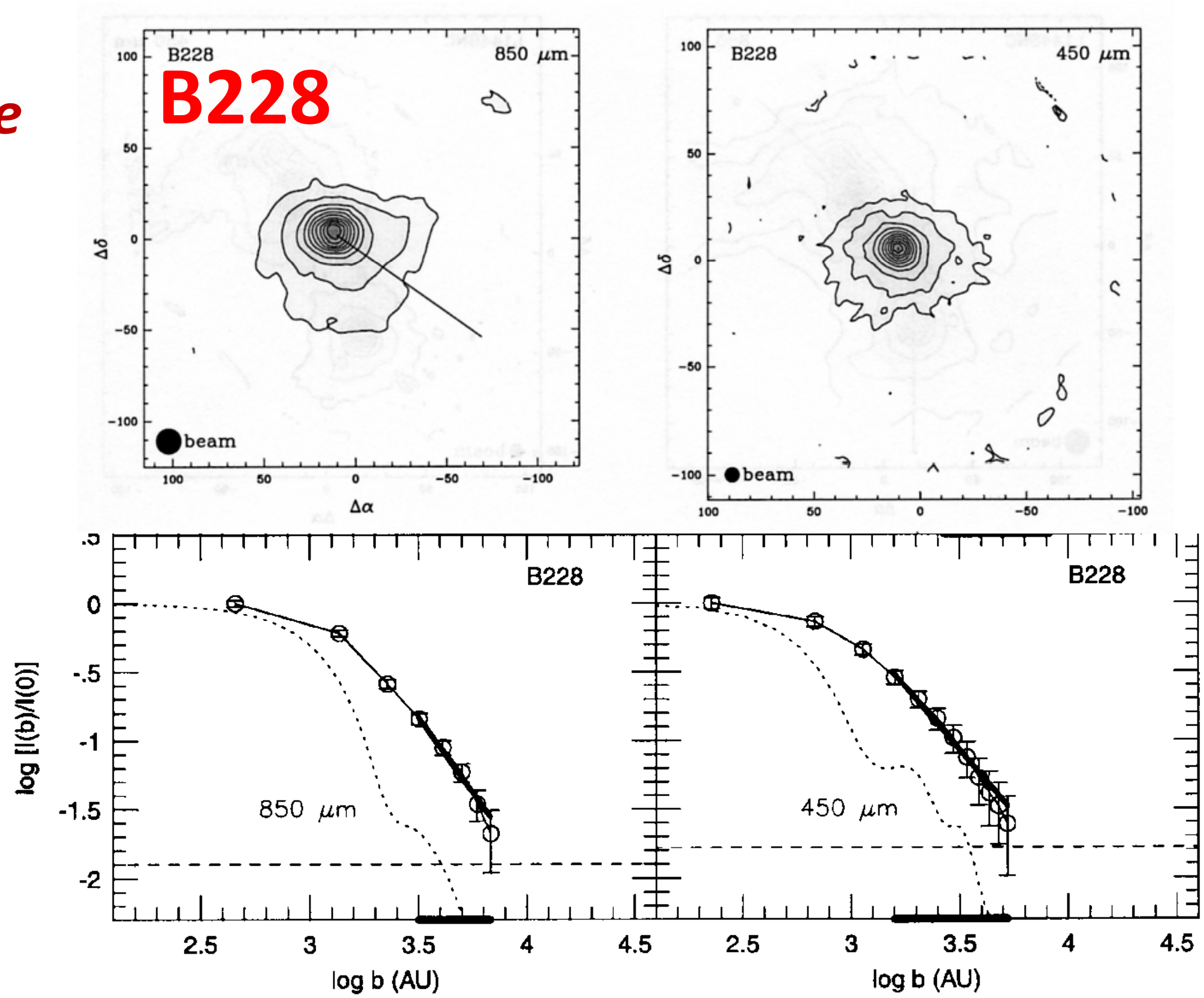

FIG. 10.—Radial profiles of Class 0 sources. The normalized intensity is plotted as a function of impact parameter, b(AU). Power-law fits are shown as bold lines. The range of the fits are indicated by the bold lines on the x-axis. The horizontal dashed lines represent the 1 σ noise level at the edge of the map. The beam profiles are shown as dashed lines in the bottom panel.

Shirley et al. 2000 ApJS 131, 249

Theoretical models

(Shu 1977, ApJ 214, 488)

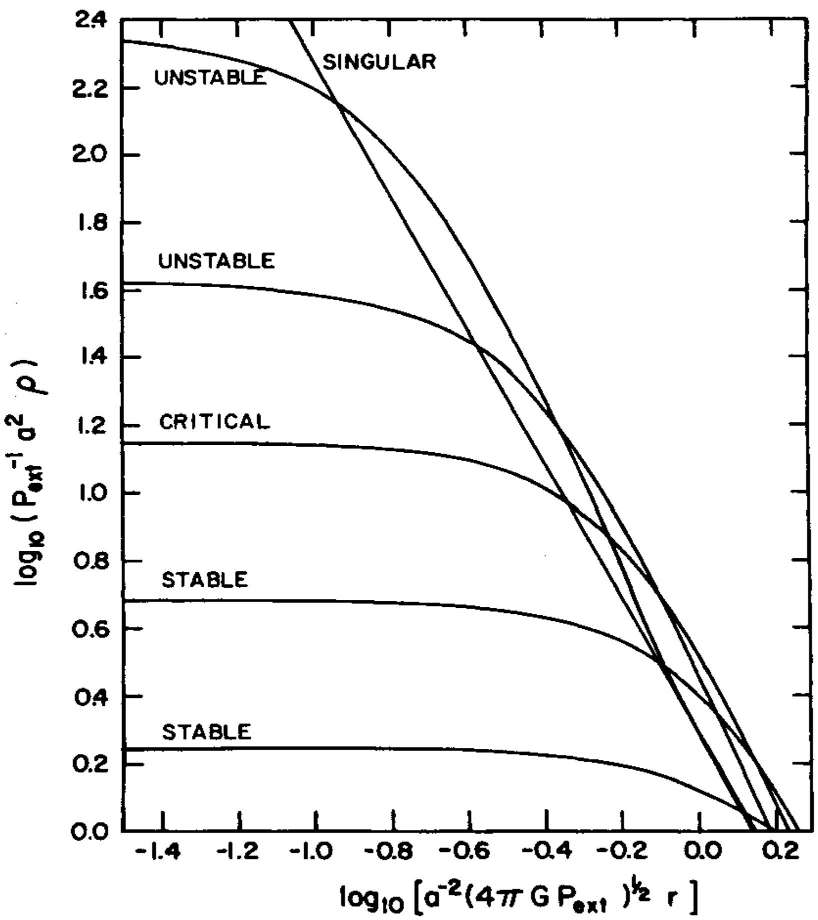

FIG. 1.—Density distributions of bounded isothermal spheres. The outer radius of each sphere is given by the intercept of the corresponding curve with the abscissa. The curve marked "critical" denotes the sphere with the maximum mass consistent with hydrostatic equilibrium at a given external pressure. Hydrostatic spheres which are less centrally concentrated than the critical Bonnor-Ebert state are gravitationally stable; those which are more centrally concentrated are gravitationally unstable. In the limit of infinite central concentration, the latter spheres approach the singular solution.

Interferometry: high resolution

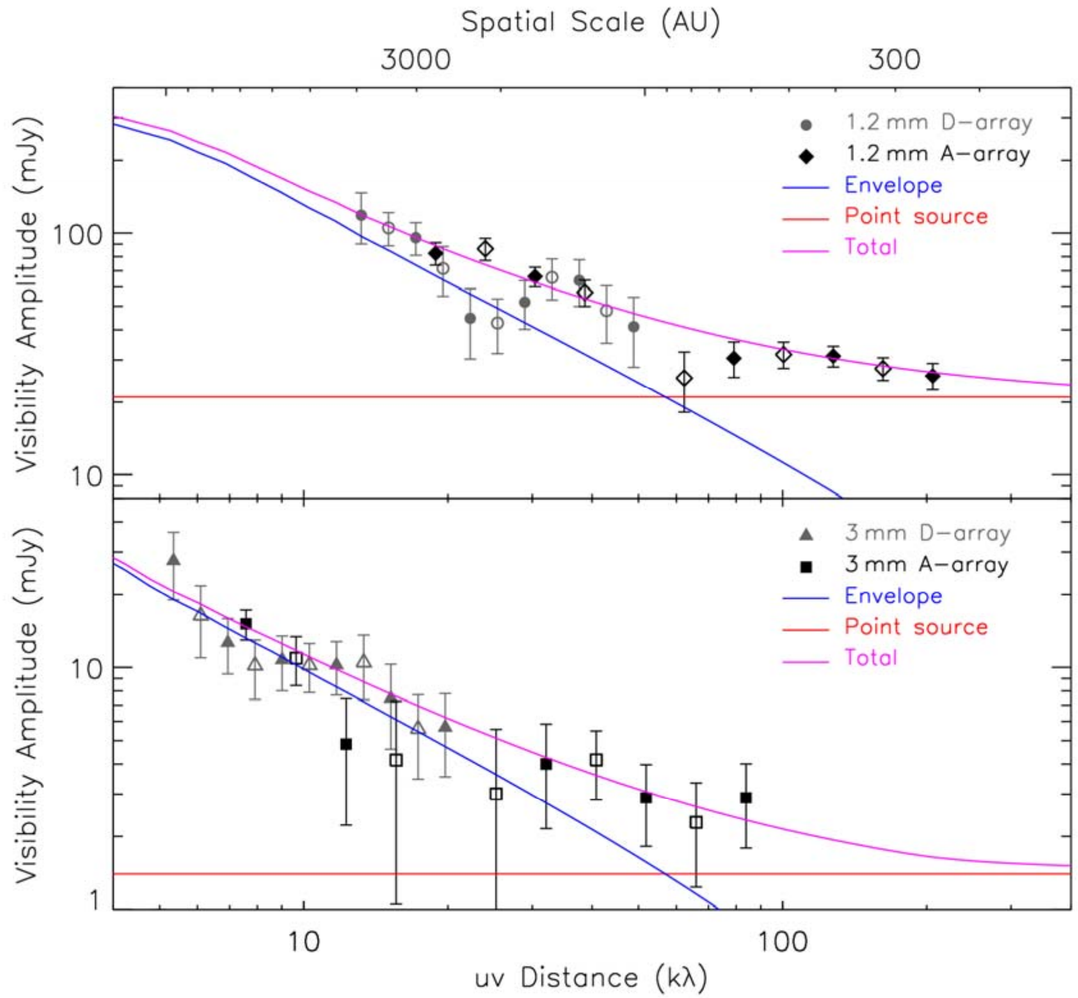

Fig. 1.— Binned visibility amplitude vs. (u, v) distance at 1.2 mm (upper panel) and 3.0 mm (lower panel) for the new IRAM PdBI observations of B335 together with the previous observations reported by Harvey et al. (2003). The derived calibration scalings have been applied to the two datasets. Note that for each dataset the bins oversample the data, and therefore the filled symbols are not completely independent from the open symbols. The best-fit model (magenta line) comprises a power law density distribution in the inner part of the envelope with $p = 1.55 \pm 0.05$ (blue line) and a point source of flux $F_{1.2\mathrm{mm}} = 21 \pm 2$ mJy at 1.2 mm (red line).

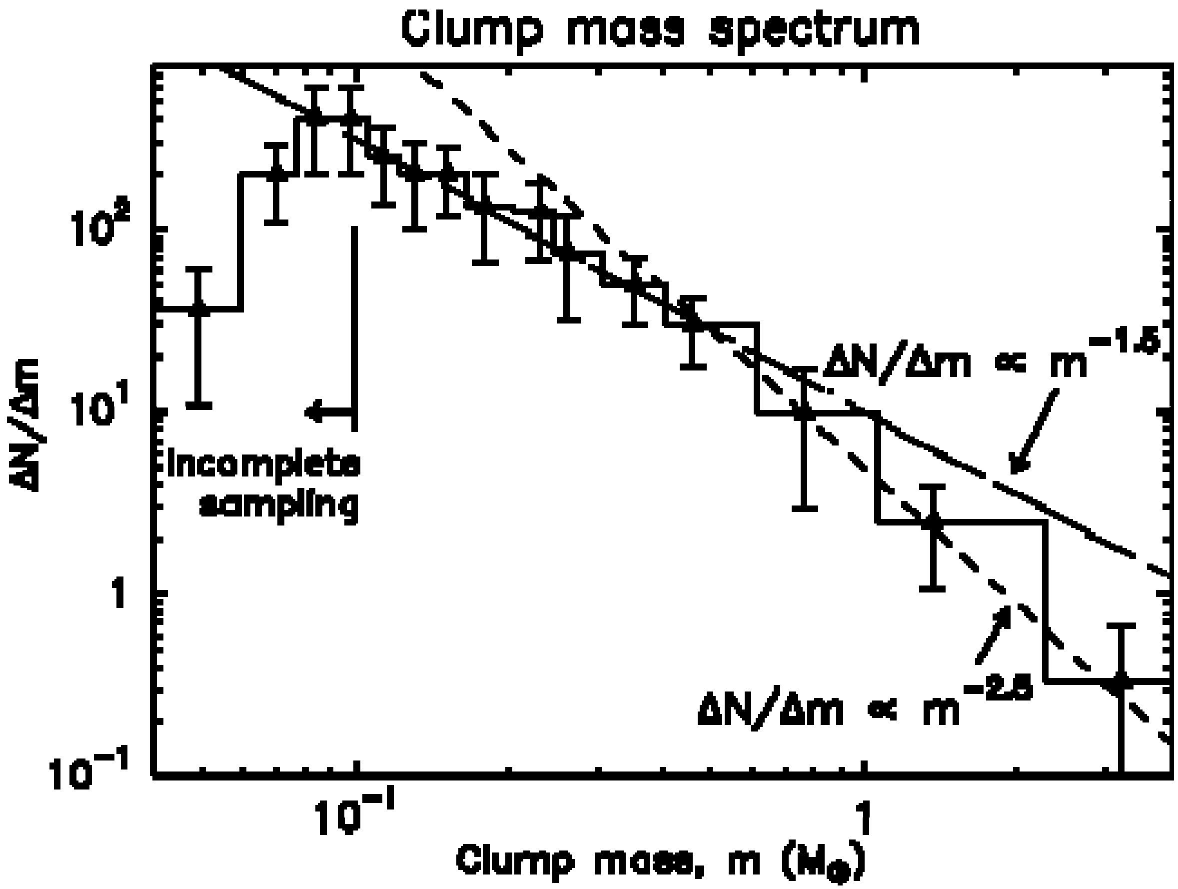

Motte et al. 1998, AA 336, 150

clump mass spectrum

$$\frac{\mathrm{d}n}{\mathrm{d}m} \propto m^{\gamma}$$

$$\gamma = -2.5 \quad \Leftrightarrow \quad \text{IMF ?}$$

Clump Mass Spectrum & IMF
1 clump → 1 star

no further Fragmentation ?

Continuum problems

- Geometry - spheres vs disks
- Calorimetric vs `true´ Luminosities
- Dust Optical Depths (Properties)
- Temperatures (Dust and Gas)

Line emission

Physical Conditions of Excitation

Cold (T_k ~ a few x 10 K ~ meV)

Large A_V (no / little external radiation) and dense (n > 10^3 cm $^{-3}$):
collisional excitations dominate level populations (if $\tau << 1$)

⇨ (low-lying) Rotational Transitions in Molecules

mostly neutrals but Cosmic Rays → molecular ions and e^-

Line emission

a) Optically *thin* lines
(optical depth *small* compared to unity)

b) Optically *thick* lines
(optical depth *large* compared to unity)

Line emission

Simplest approximation (= TE & Rayleigh - Jeans):

$\Delta T = (T_{\mathrm{ex}} - T_{\mathrm{bg}})(1 - e^{-\tau})$ [intensity $I \propto$ temperature T; On – OFF measurement]

(i)

$T_{\mathrm{ex}} = T_{\mathrm{bg}}$: no line (oohps!)

$T_{\mathrm{ex}} < T_{\mathrm{bg}}$: absorption (at least something - but difficult)

$T_{\mathrm{ex}} > T_{\mathrm{bg}}$: emission (the 'normal' case)

(ii)

$\tau << 1 \Rightarrow 1 - e^{-\tau} \approx 1 - (-1 + \tau - ...) = \tau \quad \Rightarrow \quad \Delta T \propto N_{\mathrm{mol}}$

$\tau >> 1 \Rightarrow 1 - e^{-\tau} \approx 1 \quad \Rightarrow \quad \Delta T \propto T_{\mathrm{kin}}$ [for $T_{\mathrm{kin}}/T_{\mathrm{bg}} >> 1$]

$$\int d\tau_\nu = \int \kappa_\nu dz \propto \int n_{\mathrm{mol}}\, dz \equiv N_{\mathrm{mol}}$$

$$\tau \rightarrow \infty \Rightarrow S_\nu \rightarrow B_\nu, \text{i.e. TE}$$

Effects from resolution

(a) Optically *thin* lines
(b) Optically *thick* lines

spatially unresolved

isothermal 10 K

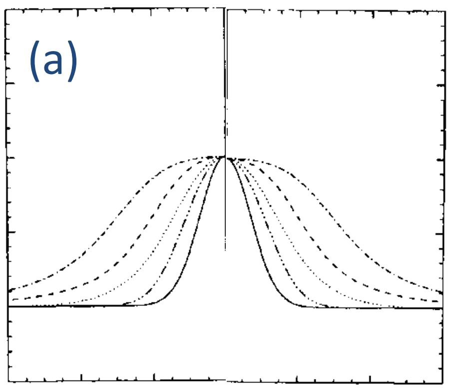

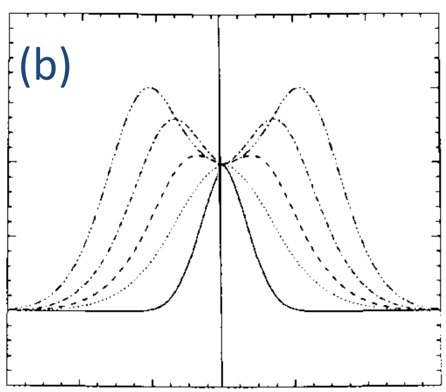

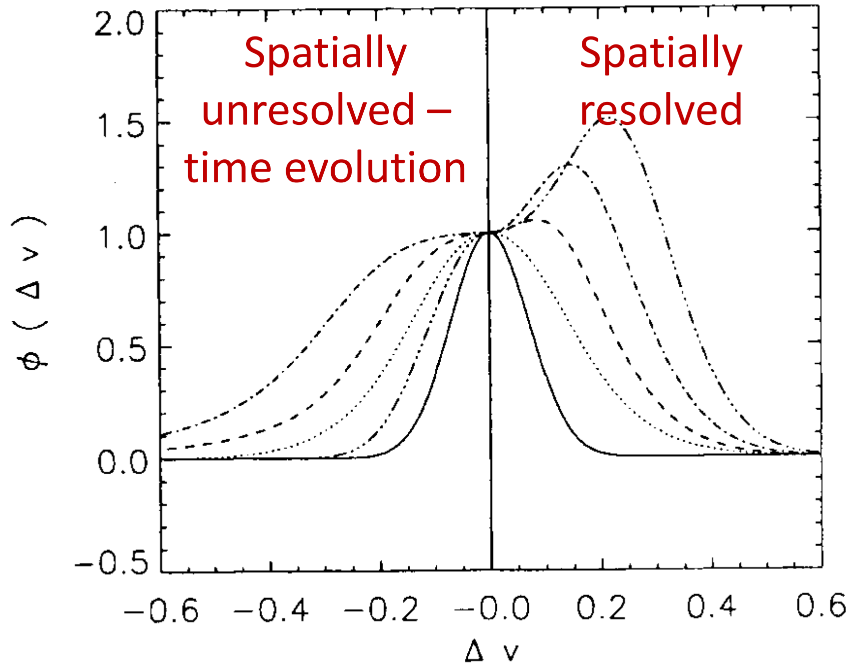

FIG. 6.—Line profiles functions for NH_3 are plotted as a function of velocity distance from line center. The line profile function presented here is a column depth of material at a given velocity along the line of sight. The profile is normalized to one at its center and the distance from line center is given in km s^{-1}. The solid line Gaussian shows a 10 K thermally broadened line profile, and the dotted line the line profile expected from the collapse of the marginally stable sphere at core formation for the physical values discussed in the text. The plot is divided into two by the vertical solid line with only half of the symmetric line profiles presented on either side. The left side shows the evolution of the line profile for an unresolved cloud. For a 4 $M_\odot$ cloud at 10 K, corresponding to a central density of 7.6×10^{-20} g cm^{-3}, the times represented are 66,000 yr prior to core formation, core formation, and 170,000 and 290,000 yr after core formation, for the dash-dot-dot-dot, dotted, dashed and dash-dot lines, respectively. The right-hand side shows the effect of beam size on the line profile. Once again, the dotted line represents the profile if the cloud is unresolved, i.e., with a beam of 5.0×10^7 cm. The dashed, dash-dot, and dash-dot-dot-dot lines represent beam sizes of 2.0×10^{17} cm, 1.0×10^{17} cm, and 4.0×10^{16} cm.

Foster & Chevalier 1993, ApJ 416, 303

Effects from optical depth

Asymmetrical Profiles

(a) Optically *thin* lines
(b) Optically *thick* lines

Carbon monoxide
CO =$^{12}C^{16}O$ (b)
and
Isotopes (a)

(a)
needs to be verified

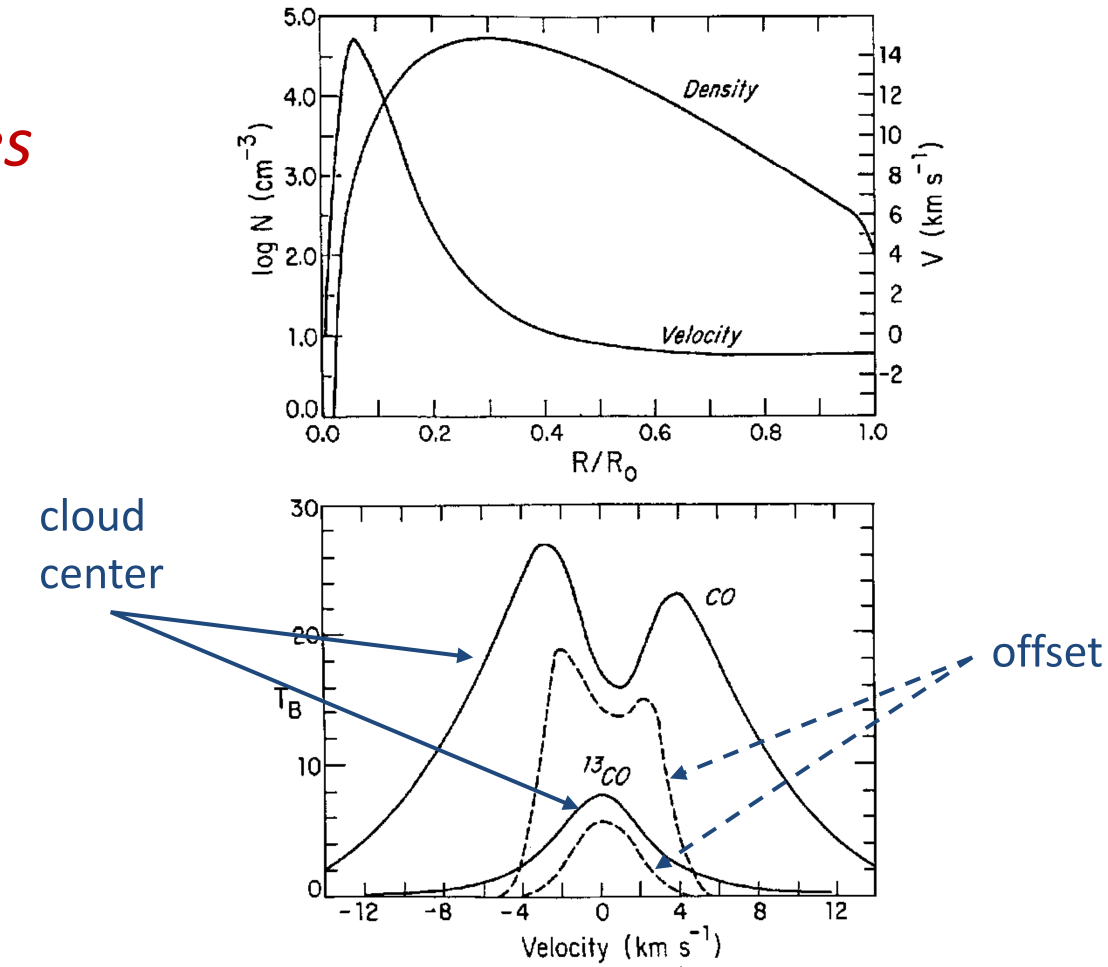

FIG. 2.—(*a*) (*upper panel*) Velocity and density distribution in a model cloud for Mon R2. (*b*) (*lower panel*) Resultant CO and ^{13}CO line profiles. Two sets of line profiles are shown corresponding to lines of sight through the cloud center (*solid lines*) and through a point ¾ pc displaced from the cloud center (*dashed lines*).

Leung & Brown 1977, ApJ 214, L73

Theoretical profiles

Asymmetrical Profiles

(b) Optically *thick* lines

for
negative temperature
gradient

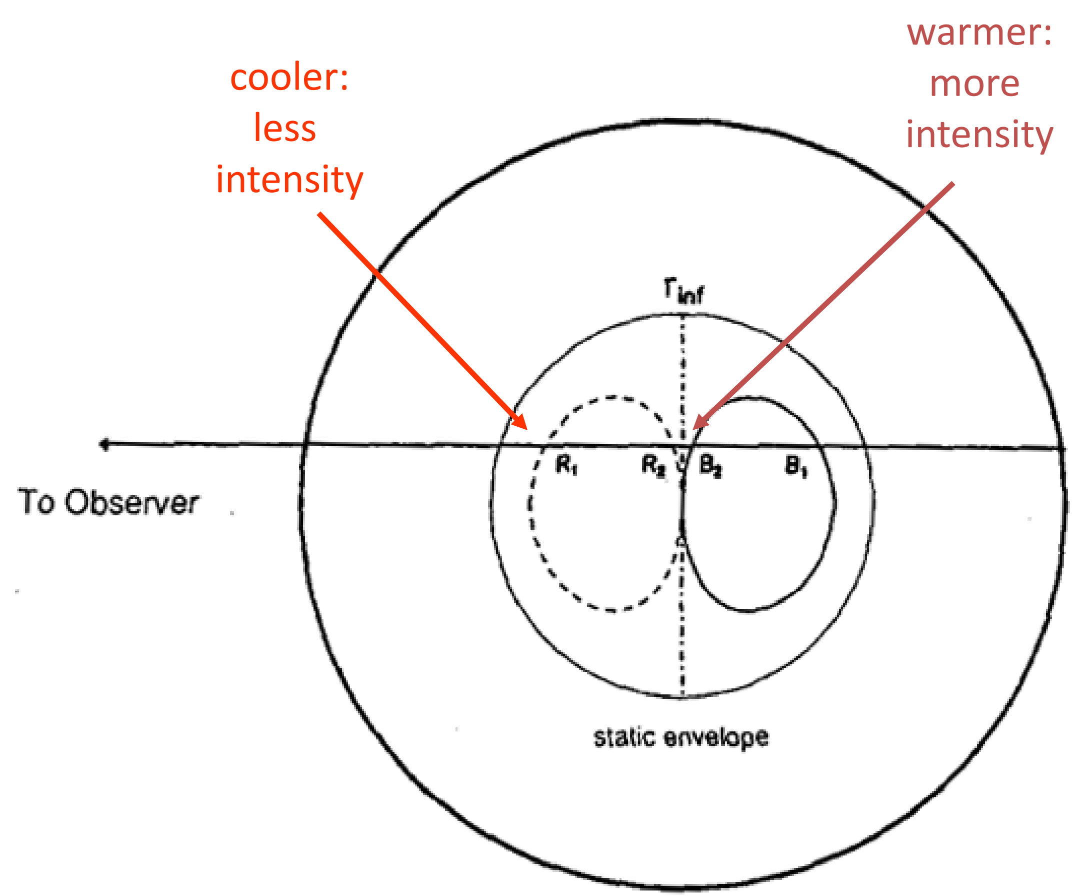

FIG. 8.—Schematic model of B335 showing the infall region inside the smaller circle. The solid line and the dashed line in the middle show the contours of equal (projected) velocity. In the case of infall, the dashed line is redshifted and the solid line blueshifted; the reverse is true for expansion.

Shu Infall

Zhou et al. 1993, ApJ 404, 232

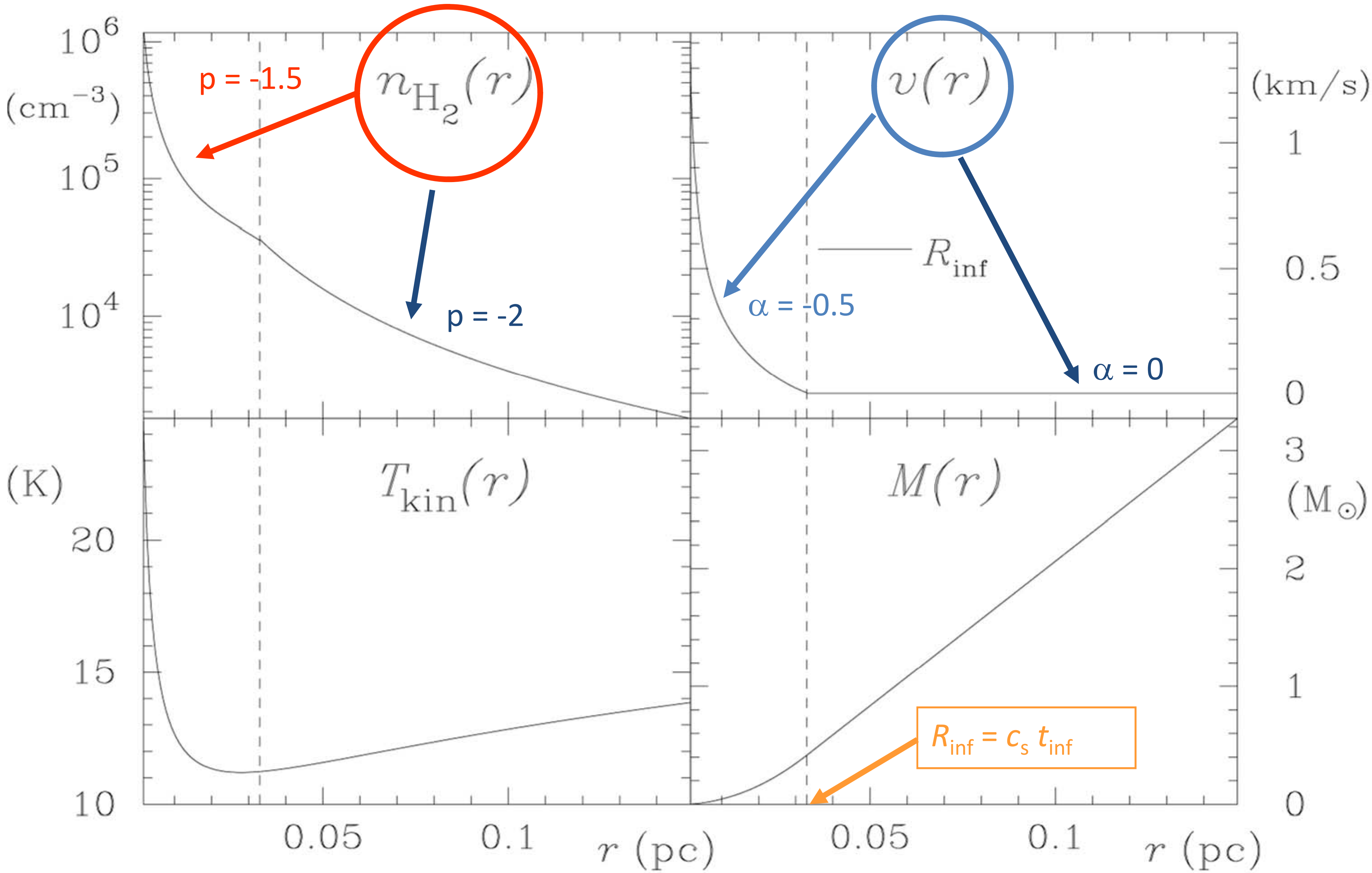

adapted from Hartstein & Liseau 1998, AA 332, 703

Model + observed profiles

Carbon Sulfide

$^{12}C^{32}S$

(main isotope)

J=2 - 1

J=3 - 2

J=5 - 4

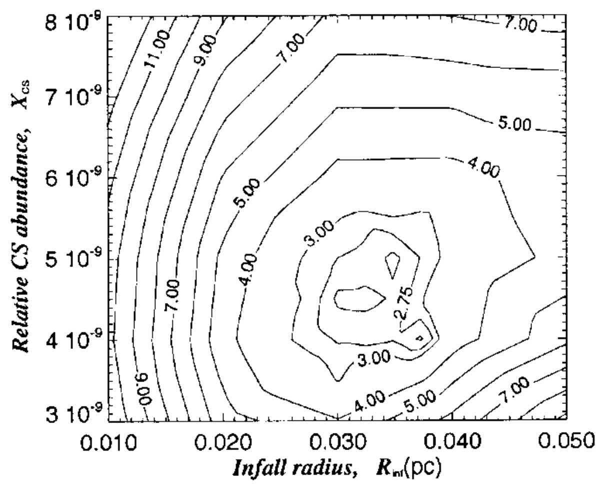

Fig. 3. The contours show the reduced χ^2 for the CS abundance (y-axis) and the infall radius (x-axis) for the Shu-type infall model of B 335 and the CS line observations by Z93. min χ^2 is found near $X_{CS} \sim 4.5\ 10^{-9}$ and $R_{inf} \sim 0.033$ pc

simply shifted, therefore, each computed line in radial velocity until it coincided with the observed profile. Keeping the position of the absorption dip fixed at $v_{LSR} = 8.35$ km s^{-1}, these shifts were -0.15 km s^{-1} for CS (2-1), (5-4) and +0.05 km s^{-1} for (3-2).

The parameter space of the model was explored between $R_{inf} = 0.01$ pc and 0.05 pc, and from $X_{CS} = 3\ 10^{-9}$ to $8\ 10^{-9}$, respectively. To evaluate the goodness of the fit between the model and the observations, we followed Choi et al. (1995) and calcu-

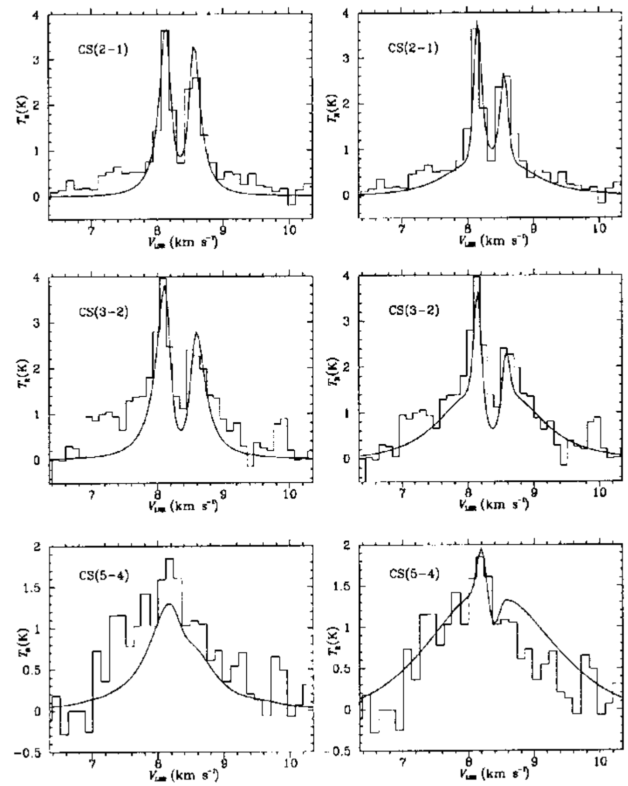

Fig. 4. Left panels: The CS lines, predicted by our best fit model of Shu-type infall in B 335 (R_{inf} = 0.0325 pc, X_{CS} = 4.5 10^{-9}, ξ_{turb} = 0.12 km s^{-1}), superposed onto the observations by Z93 shown as histogrammes. **Right panels:** The observations by Z93 are compared to a power-law model with variable microturbulence, $\xi_{turb}(r)$

Hartstein & Liseau 1998, AA 332, 703

Optical depth effects

$^{12}C/^{13}C$ ~ 60
$^{16}O/^{18}O$~ 550

Example:
Carbon Monoxide
^{13}CO
Carbon Sulfide
CS

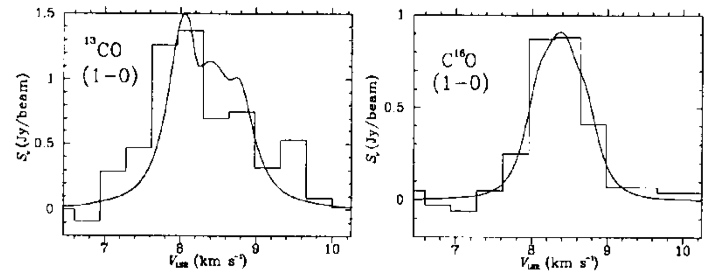

Fig. 5. Left: The ^{13}CO (1-0) line profile of the best fit CS model is shown superposed onto the interferometer observations by Chandler & Sargent (1993), displayed in histogram form. The derived ^{13}CO abundance is $X(^{13}CO) = 5\,10^{-6}$ and the theoretical profile has been scaled by the factor of 0.5 (see text). **Right:** The $C^{18}O$ (1-0) line profile ($\times 0.5$) of the model compared with the observed line shown as histogram

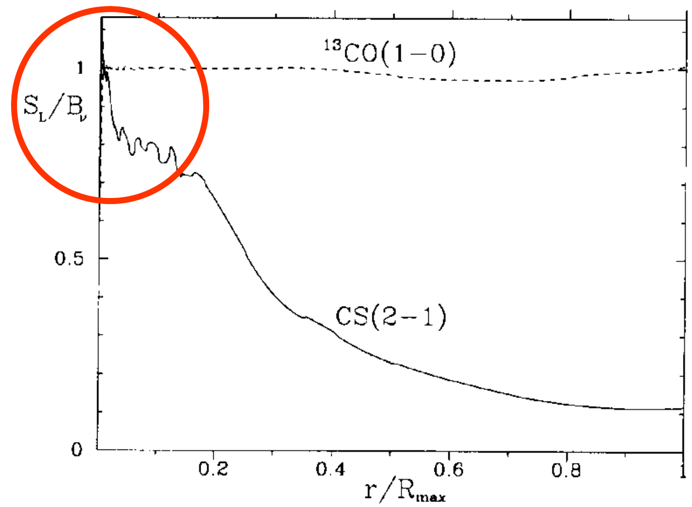

Fig. 6. The normalized line source functions for ^{13}CO (1-0) and CS (2-1) versus radial distance for the best fit CS model

Hartstein & Liseau 1998, AA 332, 703

Other diagnostics...

Current Paradigm - ?

Outflows!

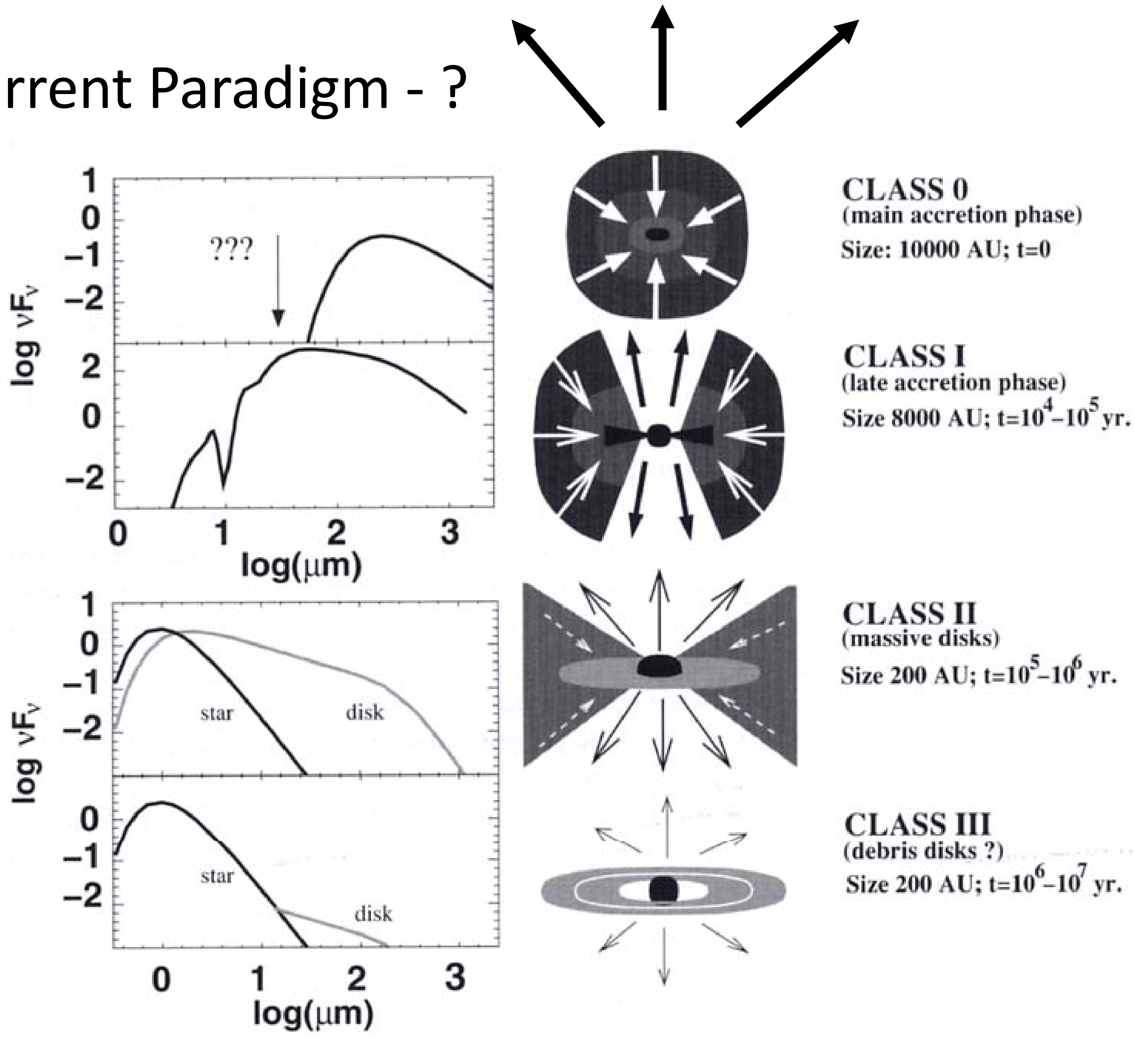

Adapted from van Zadelhoff 2002, PhD thesis

B335

See Gålfalk's PhD thesis defence on June 4!

Gålfalk & Olofsson 2007, A&A 475, 281

Conclusions

- A variety of observational techniques are exploited
- A number of collapse *candidates* have been found
- All are strong *outflow* sources
- Multiplicity is common

Open questions

- How many collapse processes do occur in nature ?
  More than one ? Which ?
- What is ***the*** `certain´ collapse tracer ?
- What spectral & spatial resolution is needed ?
- Are stars/BDs/planets formed differently ? How ?
- How are outflows generated ? Acceleration region?
- Outflows solve ang. momentum problem ? How ?